UNIVERSITY OF OKLAHOMA

GRADUATE COLLEGE

IMPROVEMENT OF SYNGAS PRODUCTION FROM WASTE RESOURCES THROUGH CHEMICAL LOOPING REFORMING USING DUAL PHASE MFe_2O_4-$Ca_2Fe_2O_5$ CATALYST

A THESIS

SUBMITTED TO THE GRADUATE FACULTY

in partial fulfillment of the requirements for the

Degree of

MASTER OF SCIENCE

By

MONICA PEGADO
Norman, Oklahoma
2024

IMPROVEMENT OF SYNGAS PRODUCTION FROM WASTE RESOURCES THROUGH CHEMICAL LOOPING REFORMING USING DUAL PHASE MFe_2O_4-$Ca_2Fe_2O_5$ CATALYST

A THESIS APPROVED FOR THE
MEWBOURNE SCHOOL OF PETROLEUM AND GEOLOGICAL ENGINEERING

BY THE COMMITTEE CONSISTING OF

Dr. Baharak Sajjadi, Chair

Dr. Karami Hamidreza

Dr. Ben Shiau

ACKNOWLEDGEMENTS

First and foremost, I would like to express my sincere gratitude to God Almighty for granting me the grace and opportunity to pursue my master's degree in a foreign country. God has been my guide throughout this challenging journey, as it was my first time as an international student and away from my family. It was a long journey that would not have been possible without Him (Psalm 127). This journey is entirely dedicated to my parents, Marcela Pegado, and Orlando Pegado, who are no longer in this world. I'm sure that wherever you are now you are very proud of me and taking care of me like always. I am truly grateful for the support and encouragement of my fiancé, family, friends, and mentors throughout my studies. Their unwavering belief in my abilities helped me persevere through the challenges and achieve my goals. Thank you again to everyone who has supported me on this journey. I could not have done it without you.

I would like to thank my mentor, Dr. Baharak Sajjadi, for accepting to work with me. Her patience and support have greatly helped me achieve my goals. It was from her that I learned what I know about renewable energy technologies. I am also grateful to my committee members Dr. Karami Hamidreza and Dr. Ben Shiau for their comments and corrections to my thesis.

During my two years at OU MPGE, I learned and expanded my knowledge of petroleum engineering and beyond, as well as how to live and respect people from different cultures. I am very grateful to everyone inside and outside OU who helped me greatly on this journey. I am particularly grateful for the support I received from Ms. Hillary Kirk, Ms. Mary Martin, and Ms. Katie Shapiro and Mr. Gary Stowe.

I am excited to use the knowledge and skills I have gained to make a positive impact on the world. I am confident that my education at OU MPGE has prepared me for a successful career in petroleum engineering.

Table of Contents

LIST OF TABLES

LIST OF FIGURES

Abstract

World consumption has demanded human beings to look for new alternatives to fossil fuel to reduce greenhouse gases effects. To supply those needs hydrogen has been studied to decrease the effect of greenhouse gases and reduce the use of fossil fuels needs. The energy sources for hydrogen production different from fossil fuels are clean, and friendly sources of energy such as biomass, wind, solar, nuclear, water. However, fossil fuels are still the main source of hydrogen production. Pyrolysis is thermochemical decomposition where biomass is decomposed into valued added materials at high temperatures in absence of oxygen. On the other hand, gasification appears to be a technique more efficient than pyrolysis; by adding gasifier agents such as steam, air, or pure oxygen where it is visible the increase on yield and quality of the bio-products. Biomass defined by any organic material prevenient from plants and animals is used on these methods due to their ecofriendly properties. On this process it is produced three different bio-products bio-oil, biochar, and syngas. Syngas is a mixture of different gases carbon dioxide (CO_2), carbon monoxide (CO), methane (CH_4), and hydrogen H_2. Hydrogen must be purified and separated from the rest of the syngas components and CO_2 captured and stored. There is a need on these hydrogen methods to add a CO_2 capture unit for hydrogen purification. This need makes a huge drawback on these technologies. Chemical looping technologies have this advantage. On a chemical looping reforming, pure CO_2 can be captured and pure H_2 produced due to the concept of two different reactors. This concept has also been applied with gasification. On the chemical looping gasification, an oxygen carrier is chosen to higher the process performance and go under many redox cycles without deactivation. A catalytic material is added to the process to accelerate the chemical reactions and increase the yield of products without being consumed during the process.

Chapter 1: Introduction

1.1 Background

Reducing greenhouse gas (GHG) emissions stands as one of the most pressing global challenges of our time. The scientific consensus underscores the pivotal role of carbon dioxide (CO_2) in driving global warming, with the combustion of fossil fuels, coal, petroleum, and natural gas—emerging as the primary source of CO_2 emissions[1]. In 2015 at the United Nations Framework Convention on Climate Change (UNFCCC) conference in Paris, it was pledged to limit global temperature rise to 1.5°C above pre-industrial levels, guiding global efforts to combat climate change, driving the search for clean, renewable energy solutions to reduce GHG emissions and alleviate climate impacts [2]. Following a temporary decrease in annual CO_2 emissions in 2020, due to the COVID-19 pandemic, a rapid rebound was observed. Emissions rose from 34 Gt in 2020 to 36 Gt in 2030[3]. This increase may be linked to factors such as the resumption of economic activity post-pandemic and a potential lack of significant changes in global energy infrastructure towards lower-carbon sources. Pushing today in renewable energy efforts is the generation of hydrogen, which presents a viable way to reduce greenhouse gas emissions and to satisfy rising energy needs. But despite its promise, several obstacles and restrictions prevent it from being widely used. Several challenges stand in the way of the effective and sustainable production of hydrogen, including high energy needs, carbon emissions during the production process, and a lack of suitable storage solutions. For hydrogen to significantly contribute to clean energy transitions, it must gain acceptance on the big sectors where its presence is currently minimal, including transportation, buildings, and power generation. Since 2000 hydrogen demand has increased. Figure 1 shows the use of hydrogen by sector and region. Hydrogen consumption witnessed robust growth across major regions, except for Europe, which experienced a notable

decline. The region's hydrogen utilization was significantly impacted by reduced activity, particularly in the chemical industry, attributed to natural gas higher prices resulted by the conflicts between Russia and Ukraine. Consequently, several fertilizer plants either scaled back production or halted operations for extended periods, leading to a nearly 6% reduction in hydrogen usage within the region. In contrast, North America and the Middle East reported substantial growth of around 7% each, effectively offsetting the decline in Europe. Meanwhile, China experienced more modest growth of approximately 0.5%, yet it remains the largest global consumer of hydrogen, accounting for nearly 30% of total usage, surpassing the United States by a significant margin. Rather than hydrogen policies, broad energy trends have been the main driver of the increase in global hydrogen consumption in recent years. This growth has mostly been seen in more established industries where the use of fossil fuels is still prevalent, such the chemical and refining sectors. As a result, its expansion has not aided in combating against climate change. Although there is a growing need for hydrogen, its use in new markets such as heavy industry, transportation, hydrogen-based fuel production, power generation and storage is still very low, accounting for less than 0.1 percent of the world's total demand. The IEA's Net Zero Emissions by 2050 Scenario (NZE Scenario), which was updated in 2023, projects that hydrogen usage will increase by 6% a year until the end of the decade. According to this trajectory, the amount of hydrogen consumed could exceed 150 Mt by 2030, with new applications accounting for roughly 40% of the growth[4]. Natural gas stands as the predominant source for dedicated hydrogen production, comprising approximately 75% of the global total, equating to roughly 70 million tons of hydrogen (MtH2) annually. This source of hydrogen production utilizes approximately 205 billion cubic meters (Bcm) of natural gas each year, representing a mere 6% of the total global natural gas consumption. Following closely behind, coal serves as the second-largest source, particularly prominent in

China, contributing an estimated 23% of global dedicated hydrogen production. This coal-based process consumes approximately 107 million tons (Mt) of coal annually, constituting about 2% of global coal usage [5].

1.2 Problem statement

Syngas can be produced through many techniques such as dry reforming of methane (DRM), steam reforming of methane (SRM), partial oxidation (POX), auto-thermal reforming (ATR) that are mainly techniques to produce syngas with fossil fuels as feedstock[6]. Where each technique has different advantages compared to others as for disadvantages. Methane undergoes a reaction with steam to generate mainly by water syngas with a stoichiometric H2/CO ratio of 3 in a high endothermic process SRM. Because of the high H_2/CO ratio and specific conditions in the process SRM compared to POX and ATR making the predominant technology for hydrogen production[7]. Ni-based catalyst is the most predominant on this technology, however, it presents constraints when used such as coke deposition, catalyst poisoning caused by the sulfur compounds even if natural gas has passed through the desulfurization pretreatment[7]. In DRM a contrast is observed,

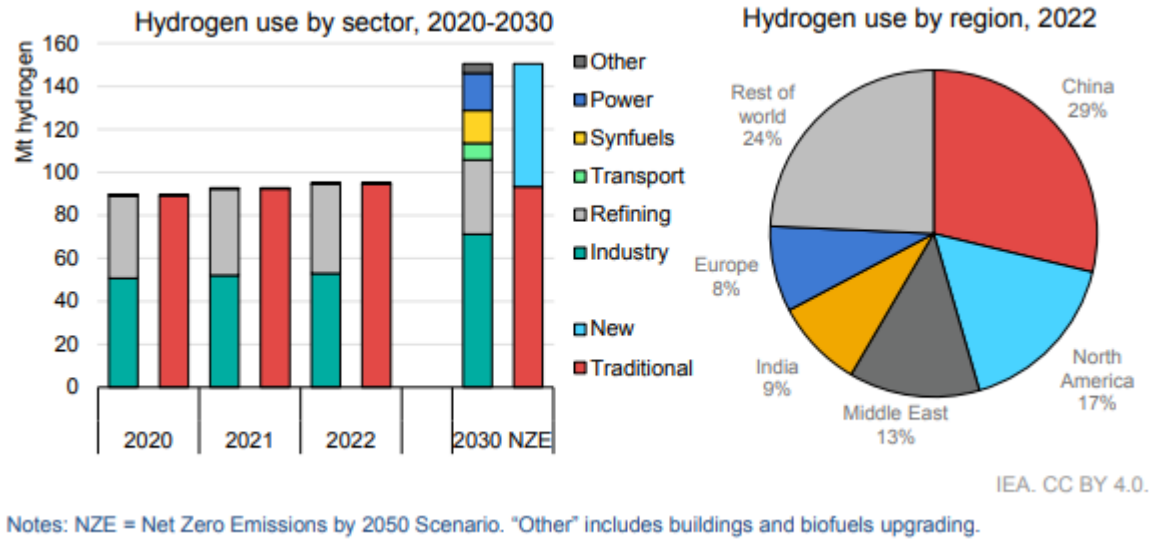

Figure 1: IEA 2023-Global demand for pure hydrogen.

methane reacts with CO_2, the oxidizing agent in high temperature reactions resulting in syngas ratio of which is suitable for the hydrocarbons from Fischer -Tropsch synthesis. Furthermore, this kind of technology needs the addition of CO_2 recovery units. Conventional methods face challenges in terms of efficiency, cost-effectiveness, and environmental impact; therefore, it is necessary to create a method that can get beyond obstacles such coke deposition, sulfur poisoning, catalyst deactivation, and the requirement to add another unit for CO_2 sequestration to produce large amounts of pure syngas. In chemical looping an oxygen carrier material that cycles between oxidation and reduction states, transporting oxygen from air reactor to the fuel reactor without directly involving air in the fuel conversion process. This thesis aims to address these issues by investigating the use of dual phase MFe_2O_4-$Ca_2Fe_2O_5$ catalysts in chemical looping reforming to improve syngas production efficiency and environmental sustainability. Furthermore, for a completely sustainable syngas production biomass recycled wood railroad ties are going to serve as fuel for the chemical looping reforming since they present amount of carbon, hydrogen and oxygen that are useful to produce syngas.

1.3 Research Objectives

To improve the production of syngas dual-phase catalysts in a chemical looping reforming will be investigated. In a fixed bed reactor, the activity and performance of $Ca_2Fe_2O_5$, $Ca_2Fe_2O_5$+$CuFe_2O_4$, $Ca_2Fe_2O_5$+$CoFe_2O_4$, and $Ca_2Fe_2O_5$+$NiFe_2O_4$ dual phase catalysts will be investigated. The yield of syngas gas can is influenced by many variables, on this thesis it is going to be investigate:

1. **Evaluate the Feasibility of Utilizing Discarded Railroad Ties for Energy Conversion**
    - Investigate the potential of using discarded railroad ties as a feedstock for energy conversion by converting the discarded railroad ties into valuable products.

2. **High Purity Hydrogen Production via Chemical Looping Reforming (CLR)**
    - Study the feasibility of utilizing a $Ca_2Fe_2O_5$-based brownmillerite structures for high-purity hydrogen production through the CLR process.
3. **Development and Evaluation of Dual-phase Oxygen Carriers**
    - Synthesize and characterize a mixing of $Ca_2Fe_2O_5$ combined with $CuFe_2O_4$, $CoFe_2O_4$, and $NiFe_2O_4$ to assess how the oxides type and concentration impact reactivity with biomass, syngas production, and hydrogen enrichment and purity.
4. **Optimization of CLR Operating Conditions**
    - Investigate the influence of key operating parameters, including temperature and water injection rate to maximize product yields and quality, particularly on the production of high-purity hydrogen.
5. **Develop a valuable application for biochar**
    - Assess the influence of biochar on asphalt's properties at high temperatures, particularly emphasizing its role in enhancing resistance to rutting and cracking on modified binder.

1.4 Thesis Outline

This thesis is organized in the following order:

Chapter 1: Introduction - This chapter provides a succinct overview of the challenges and constraints associated with hydrogen production and offers a global perspective on the status of hydrogen technology. It briefly highlighted the challenges associated with hydrogen technologies. The background is followed by the problem statement, research objectives, and thesis organization the design of chemical looping reactors and explain about the model developed in this study to simulate the fluid flow pattern, instabilities, and key variables in CL reactors. The objectives of the project are formed, and the outline of the thesis is clarified.

Chapter 2: Literature Review - This chapter's first section offers a comprehensive overview of the literature on the categorization of hydrogen production methods and the significance of contemporary methods for creating hydrogen, such as chemical looping technology. As a result,

the main branches of chemical looping technology are examined, with a special emphasis on the system ability to produce hydrogen. This chapter's second section provides a succinct overview of perovskites' structural characteristics.

Chapter 3: Methodology - In this chapter, railroad ties biomass preparation steps are presented from grounding to the final product for syngas production. The dual phase catalyst synthesis by sol gel method for catalyst synthesis is presented. Fundamental equations for syngas yield and syngas components and reactor set up and procedures are also discussed and presented. Furthermore, catalyst characterization XRD, FTIR, SEM-EDS, TEM-EDS, BET, and elemental analysis are presented.

Chapter 4: Results and Discussions- This chapter is divided and presented in three parts. The first section includes catalyst characterization, understanding highlighting homogeneity, surface area, porous structures, how stable is the catalyst after 2-3 cycles and studying the effect of catalyst on the chemical looping process. The second section includes pyrolysis results and parameters analysis such as temperature and catalyst effect. The third part of the chapter discusses the chemical looping results including the temperature and catalysts effects and a comparison between pyrolysis and chemical looping.

2 Chapter 2: Literature Review

2.1 Introduction

Since industrialization, human beings have relied on non-renewable energies to generate heat and electricity. With new living standards and therefore high energy consumption, a new era is marked by growing environmental concerns, negative climate impacts, and a desire for sustainable solutions [8]. It was reported in 2022, that the utilization of fossil fuels resulted in the release of 11.2 Gt of CO_2 emissions [4]. Unfortunately, it is expected that the global world energy consumption will continue to increase through 2050. In consequence, the significance of renewable energies has never been more eminent since the greenhouse gas emission keep increasing. Renewable energies, often referred to as clean or green energies, are a big alternative to fossil fuel since they occur naturally and it is in constantly renovation, thus, providing an environmentally friendly and sustainable alternative to conventional fossil fuels. Biomass stands out due to low green gas emissions, a wide source, and high hydrogen content[9].

Driven by the harmful effects of greenhouse gases and the potential scarcity of fossil fuels, the world is searching for new ways to power our needs. While renewable sources like wind, solar, and hydro are attractive, their inconsistency and dependence on location limit their ability to fully meet current global energy demands. Fortunately, hydrogen emerges as a promising alternative energy source[10]. According to Modern Chemistry, hydrogen composes 75% of the elements on earth. The most abundant element on earth stands as the primary carbon-free energy carrier, though commonly occurring alongside other elements. For a long time, hydrogen has been considered a renewable energy source that is environmentally friendly[11]. According to the International Energy Agency (IEA) 76% of hydrogen is mainly produced from natural gas, 22% from coal, and 2% from water electrolysis. When it comes to hydrogen production either by renewables

specifically biomass or fossil fuels, a combination of gases is produced called syngas. Syngas is a mixture of gases primarily composed of hydrogen and carbon monoxide generated regardless of the hydrogen technique [12]. Due to its attraction as a clean and versatile energy carrier with the potential to revolutionize various sectors in the transition towards a low-carbon economy hydrogen has many applications [13] figure 2:

- Chemical component to produce ammonia (NH3) used in fertilizers.
- Clean and low-carbon fuels for transportation.
- Food and pharmaceutic industries as a hydrogenation agent.
- Chemical components in petrochemical and refining products.

Various methods are considered for hydrogen generation, categorized as either conventional or renewable. On the conventional technologies natural gas and coal are used as feedstocks which produce more CO_2, while renewable technologies utilize biomass, solar, and wind sources. These processes produce hydrogen, which can be stored, transported, and utilized for energy generation, as shown in figure 2. Hydrogen is colorless and odorless; however, it can be classified by the colors which is another alternative categorization of hydrogen. On Ajanovic et al [14] it is described the different hydrogen color classification (Figure 3) such as Grey Hydrogen, produced predominantly through steam reforming of natural gas or coal, represents the most prevalent method globally, contributing over 40% of hydrogen production. However, its environmental footprint is significant, characterized by high CO_2 emissions. Blue Hydrogen, a cleaner alternative to grey hydrogen, incorporates carbon capture technology to mitigate emissions. Despite this improvement, challenges persist, including methane leakage and the need for effective CO_2 storage solutions. It is often viewed as a transitional solution towards greener alternatives. Turquoise Hydrogen, an emerging technology utilizing methane pyrolysis, offers a promising pathway to

reduce emissions. By generating solid carbon as a byproduct instead of CO_2, it presents a more environmentally friendly option. However, its development is still in its infancy stages. Purple/Pink Hydrogen leverages nuclear power for electrolysis, providing a potential solution to reduce nuclear plant shutdowns and offering energy storage capabilities. This approach holds promise for efficiency enhancements and diversification of energy sources. Green Hydrogen, hailed as the goal, is produced via water electrolysis using renewable electricity sources such as wind and solar. Recognized for its minimal emissions and environmental sustainability, it stands out as a truly clean energy solution. Key technologies include alkaline, polymer electrolyte membrane (PEM), and solid oxide electrolyze cell (SOEC), each offering unique advantages in terms of cost, efficiency, and urban compatibility.

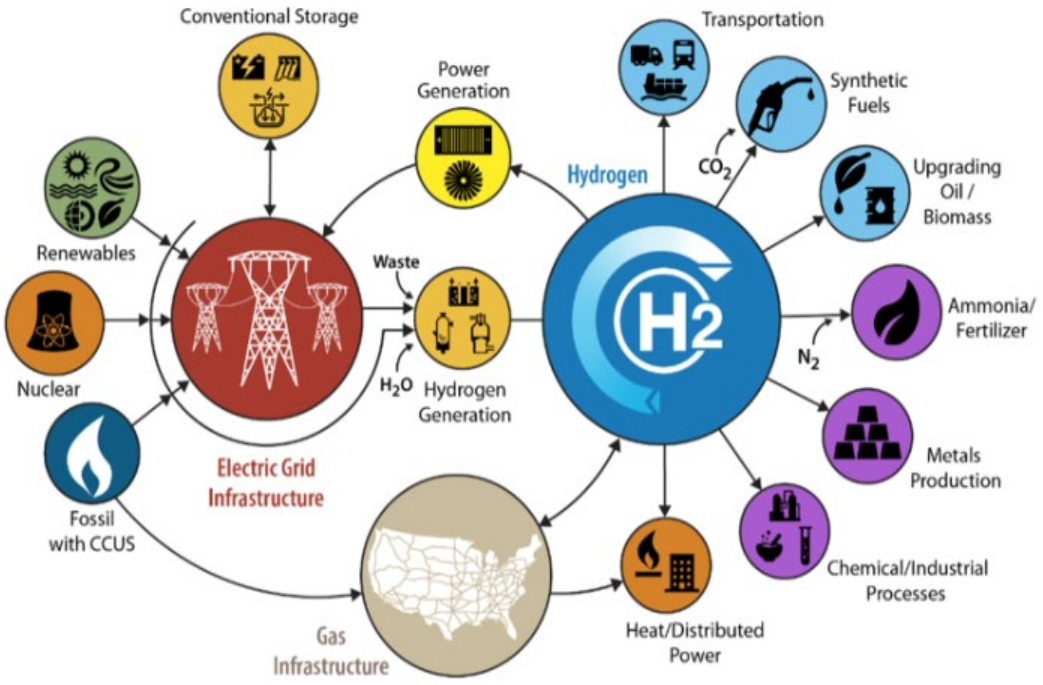

Figure 2. Diverse hydrogen applications and different hydrogen sources, conventional and renewables.

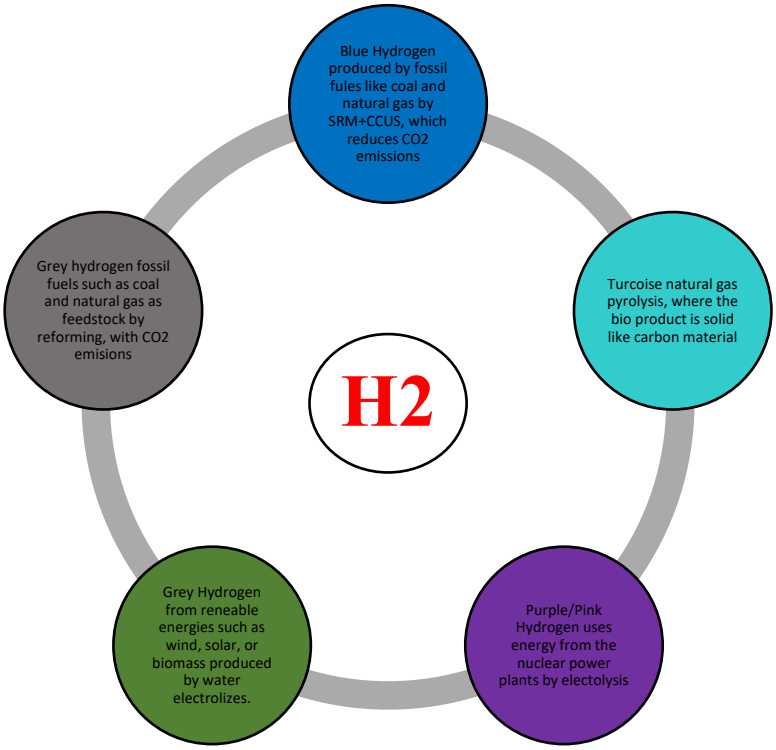

Figure 3. Hydrogen colors. Numerous investigations have demonstrated that there are many ways to categorize hydrogen [8-10]. Furthermore, brown hydrogen and black hydrogen are also considered both using gasification technology resulting in high emission of CO2. Brown hydrogen is considered as feedstock the brown coal also known as lignite and Black Hydrogen considered feedstock the black coal.

2.2 Hydrogen Production from fossil fuels

Hydrogen, as a clean and versatile energy carrier, holds tremendous potential to play a pivotal role in the transition towards a sustainable energy future. One of the primary methods for producing hydrogen on a large scale is through the utilization of fossil fuels (figure 4), namely natural gas and coal. More precisely, 48% of hydrogen produced to date came from natural gas, 30% from naphtha and heavy oils, and 18% from coal[6]. Hydrogen production from fossil fuels, particularly through processes such as steam methane reforming (SMR) and coal gasification, has been instrumental in meeting the growing demand for hydrogen across various industrial sectors. Fossil fuel-based hydrogen production processes have long been established and are known for their efficiency, reliability, and cost-effectiveness. These methods leverage the abundant reserves of

natural gas and coal, making them readily available feedstocks for hydrogen generation. However, despite their advantages, fossil fuel-based hydrogen production poses environmental challenges due to the release of carbon dioxide (CO_2) and other greenhouse gases during the production process. Due to the negative impact of the fossil fuel-based hydrogen, the renewables energies have been used as an alternative to fossil fuel usage consequently the environmentally friendly and pollution-free techniques are employed (figure 5)[15].

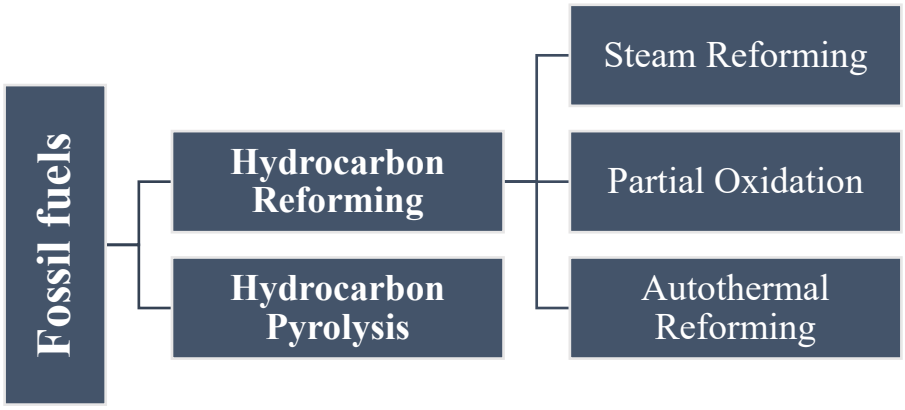

Figure 4. Hydrogen production technologies from fossil fuels.

Biomass, one of the renewable sources of energy, refers to organic matter derived from living organisms including both plant and animal materials that were previously alive. Because of its low carbon dioxide emissions, wide availability, renewability, and high hydrogen content, it serves as a cost-effective and abundant resource for producing alternative transportation fuels, electricity, heat, and valuable chemicals[16]. There is a variety of biomass like solid waste, agricultural residues, wood, and animal manure. It can be converted into biofuels, electricity, heat, biochemicals through conversion processes namely biochemical and thermochemical conversion techniques[17]. Biochemical conversion includes methods such as fermentation and anaerobic digestion. In these methods microorganisms, enzymes or bacteria are used to break down cellulosic materials, leading to the production of biofuels and various chemicals. On the other hand, thermochemical conversion involves the use of elevated temperature to convert organic material into different kinds of bioproducts. In contrast to biochemical conversion, thermochemical conversion does not rely on chemical agents but rather employs heat as a catalyst for chemical reactions. Thermochemical conversion can include various technologies, such as combustion, gasification, and pyrolysis.

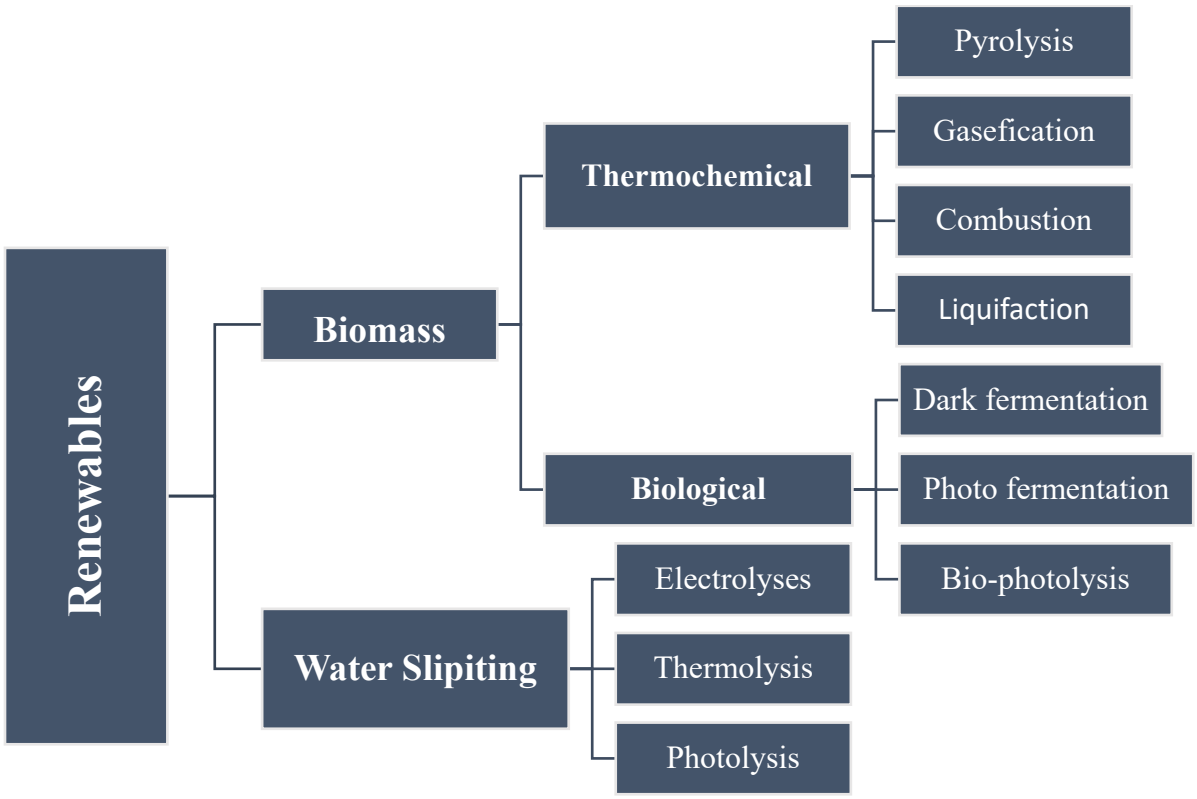

Figure 5. Hydrogen production technologies from renewables.

2.2.1 Steam Methane Reforming (SMR)

The process of steam methane reforming (SMR) is the most popular method for producing hydrogen in the world because of its high conversion rate and attractive economics. These come from the high process efficiency (74–85%) and lower capital cost in contrast to other production technologies[18]. The main step in the steam reforming (SR) process is the catalytic conversion of steam and hydrocarbons into carbon oxides and hydrogen. The production of reforming or synthesis gas (syngas), the water-gas shift (WGS) reaction, and the purification of gases using gas purification or methanation processes are some of the crucial stages involved seen in figure 6. On the natural gas steam reforming process, the first step involves pre-treating natural gas to eliminate sulfur compounds through desulfurization, a crucial measure to prevent catalyst poisoning,

typically employing Nickel-based catalysts[19]. Simultaneously, water is heated to generate steam. Subsequently, both components are introduced into the reformer along with methane and heat. Within the reformer, operating at temperatures ranging from 700 to 900 degrees Celsius, a chemical reaction (reaction1) occurs where methane reacts with steam to yield hydrogen and carbon monoxide, the primary constituents of syngas. Following reforming, the gas mixture is directed to the water gas shift unit (WGS), where carbon monoxide interacts with steam, leading to the production of additional hydrogen and carbon dioxide. Finally, the hydrogen undergoes purification in the last unit, employing a preferred method as seen in figure 6 [20]. The two main reactions that typically occur during this process are the water gas shift (WGS) (reaction. 1) and the reformer steam (reaction. 2):

$$CH_4 + H_2O \rightarrow CO + 3H_2 \qquad \textbf{R1}.$$

$$CO + H_2O \rightarrow CO_2 + H_2O \qquad \textbf{R2}.$$

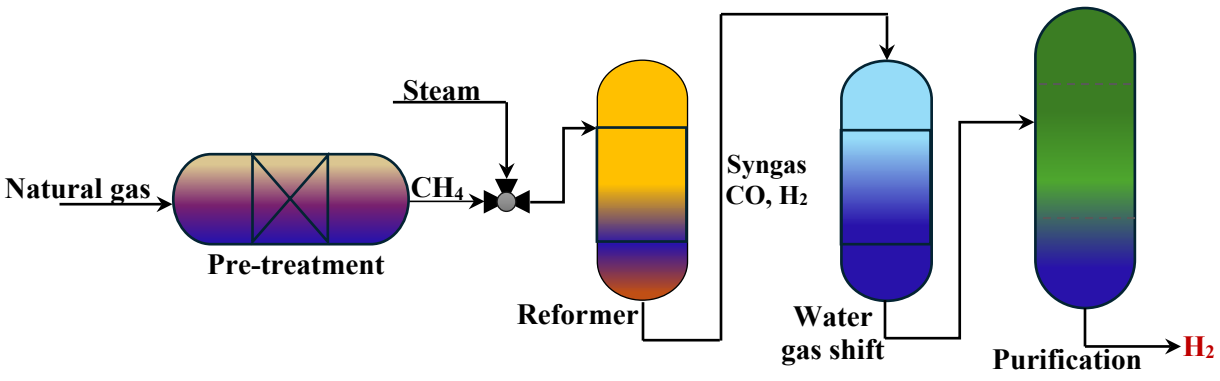

Figure 6. Steam Methane Reforming.

2.2.2 Partial Oxidation

The partial oxidation (POX) method is similar to SMR; however, the conversion occurs basically with reactions of hydrocarbon, steam and oxygen converted into carbon monoxide and hydrogen. Following the removal of sulfur on the desulfurization unit, a process involving the use of pure oxygen is employed to partially oxidize the hydrocarbon feedstock. The resulting syngas undergoes subsequent treatment steps similar to those applied to the product gas generated in the steam reforming process. This process is used for heavier feedstocks such as heavy hydrocarbons, oil wastes, naphtha, coal, and methane to hydrogen [21]. The operation temperature for this process varies from 1150-1315c in non-POX and 950c for the catalyst-POX[6]. On the catalytic-POX, catalysts serve to reduce operational temperatures. Therefore, transition metals from groups 8, 9, and 10, including nickel (Ni), cobalt (Co), iron (Fe), ruthenium (Ru), rhodium (Rh), palladium (Pd), iridium (Ir), and platinum (Pt), are commonly utilized as catalysts for partial oxidation of methane (POM) reactions. Among these, supported nickel, cobalt, and noble metal catalysts (such as Ru, Rh, and Pt) have been extensively investigated. Additionally, alternative catalyst systems like pyrochlore oxides (e.g., Ln2Ru2O745), perovskite oxides (e.g., LaNiO3, LaNixFe1-xO3), and hydrotalcite-type materials (e.g., Ni-Mg-Al hydrotalcites) have been explored as catalyst precursors for POM reactions, particularly in the partial oxidation (POX) method[22]. However, effectively managing temperature remains challenging due to the formation of coke and hot spots resulting from the exothermic reactions involved. In natural gas conversion, catalysts primarily rely on nickel or rhodium; however, nickel exhibits a pronounced tendency to coke, while the escalating cost of rhodium presents a significant drawback. This presents a notable disparity compared to the implementation of catalysts in the partial oxidation method[23].

$$CH_4 + \frac{1}{2}O_2 \rightarrow CO + 2H_2 \qquad \textbf{R3.}$$

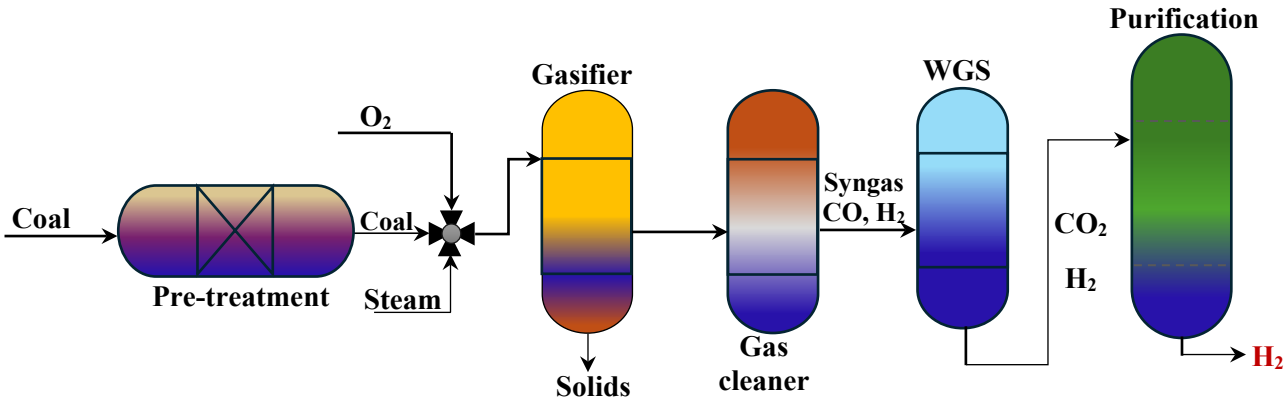

Figure 7. Partial Oxidation method.

2.2.3 Autothermal Reforming

Autothermal reforming (ATR) of methane is a combination process that combines steam reforming and partial oxidation. In this method, the heat needed for reforming is generated by the combustion of the feed in an adiabatic reactor[24]. Consequently, partial oxidation produces the required thermal energy, while steam reform enhances hydrogen production[6]. This catalytic reforming process involves injecting three reagents (CH4, H2O, and O2) into the reformer simultaneously, facilitating reforming and oxidation reactions[25]. For methane feedstock, the process efficiency typically ranges between 60-75%, with an optimal temperature of 700°C, steam to carbon (S/C) ratio of 1.5, and oxygen to carbon (O2/C) ratio of 0.45. The hydrocarbon feedstock, mixed with steam, enters the reformer where it reacts with oxygen from a burner, undergoing partial oxidation and steam reforming at high temperatures. Some methane reacts with oxygen to produce heat, while the remaining methane reacts with steam to yield hydrogen and carbon oxides. This reaction can be seen in reaction (4). ATR of methane aims to conserve

energy by generating the required thermal energy through the partial oxidation of methane. This self-sustaining process is termed autothermal, as it consumes the thermal energy it produces[26].

$$CH_4 + 3/2O_2 \rightarrow 2H_2O + CO \qquad \boldsymbol{R4.}$$

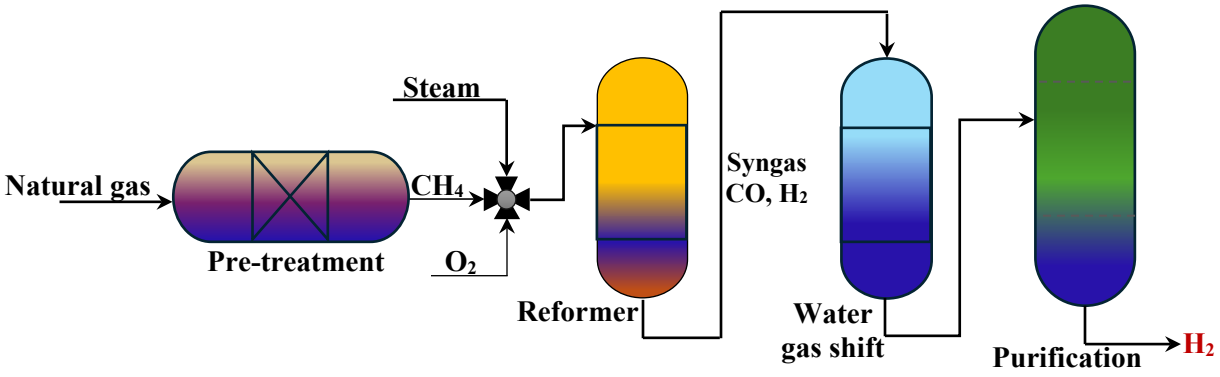

Figure 8. Auto Thermal Reforming.

2.3 Chemical Looping for Hydrogen Production

Chemical Looping Gasification (CLG) stands as an innovative approach for producing syngas, originating from the concept of Chemical Looping Combustion (CLC) initially proposed by Lewis and Gilliard in 1954 in their work titled "Production of pure carbon dioxide"[27]. CLC was originally conceived as the technology to capture carbon dioxide. In the process, H_2 is naturally isolated from a COx stream, eliminating the need for extra separation costs. This separation process is facilitated by metal oxides that transport oxygen from an oxygen-rich source (such as steam, air, or oxygen) to the fuel, known as oxygen carriers. These carriers are typically composed of metal oxides, primarily Ni, Cu, Co, Mn, and Fe. In each phase of the process, the oxygen carrier is initially reduced while converting fuel into syngas or complete oxidation byproducts (CO_2 and

H_2O). Subsequently, their lattice oxygen is restored by reacting with steam, producing pure hydrogen[28]. Additionally, CLG shows advantages over conventional gasification methods, including reduced emission of pollutants (CO_2), decreased energy loss, and the production of high-quality syngas.

Chemical looping methods offer an intriguing alternative for electricity and/or hydrogen generation when paired with CO_2 collection, which is more efficient than traditional CO_2 capture technology [29, 30]. Chemical looping is a method for addressing CO_2 collection and low NOx emissions [31] and it enables the low-cost production of compounds such as syngas and H_2. The chemical looping reaction strategy involves dividing a reaction into numerous auxiliary responses, which are helped by solid intermediates known as "oxygen carriers", which alternate between reacted and regenerated states. The phrase "chemical looping" refers to the process of breaking down a reaction into discrete reactions in which the intermediates are in a continuous cycle of reaction and regeneration. The purpose of this procedure is to allow these reactions to take place in a way that maximizes system efficiency while also making it simple to separate the necessary products, making the process more efficient and cost effective. In 1987, Ishida et al. [32] were the first to coin the phrase "chemical looping" to describe a method of using a metal oxide as an intermediate mechanism to accomplish a cyclic oxidation-reduction reaction process for power generation. A solid is employed as an oxygen-carrier (OC) in chemical looping processes to convert the fuel, and the solid is then oxidized with air in a continuous cycle. The oxygen carrier, which is frequently comprised of metal oxides, nitrides, hydrides, and sulfides, acts as a reservoir for oxygen donation and regeneration. A redox loop is formed in a conventional chemical looping process, consisting of two or more reduction and oxidation stages. An oxygen carrier or redox catalyst initially transfers the most basic form of its lattice

oxygen [33]. When the reduced oxygen carrier is exposed to an oxidant to replace its lattice oxygen, a two-step redox cycle is completed.

2.4 Chemical Looping Technologies (CLT)

Since the beginning of industrialization, there has been an increase in the amount of carbon dioxide in the atmosphere, with a notable acceleration throughout the last century. There is broad global agreement that reducing carbon emissions is essential as the world struggles with the severe effects of climate change [34]. Chemical looping techniques offer an attractive alternative for CO_2 capture technology when it comes to producing hydrogen and/or power. This strategy outperforms traditional CO_2 capture techniques in terms of efficiency[35]. Chemical looping technology is a versatile and effective process intensification technique that uses solid reaction intermediates to divide chemical reactions into many sub-reactions. It allows one to reduce costs and emissions by optimizing the allocation of materials and energy. This method, which was first described as "chemical looping combustion," was first used to produce electricity and capture CO_2[36]. Its special ability to spatially separate fuels from air improves combustion and makes CO_2 extraction easier. With the use of chemical intermediates such as metal oxides, this method breaks down complicated reactions into manageable steps that may be carried out in different reactors. This novel method reduces the amount of time that inert components in feedstocks come into direct touch with the intended product, which lowers purification expenses[37]. A comprehensive comparison evaluating the performance of two distinct power plant designs was carried out in a study by B. Erlach et al[30] . One of the designs used chemical-looping combustion integrated coal gasification combined cycle with carbon capture (CLC IGCC), while the other used a conventional IGCC design with pre-combustion carbon capture using physical absorption. The CLC-IGCC system had a greater efficiency of 37.7%, whereas the IGCC system

demonstrated a low efficiency of 34.9%. Highlighting the technique of chemical looping as a promising method.

2.4.1 Chemical Looping Combustion (CLC)

The concept, initially proposed in a patent by Lewis and Gilliland and later termed by Ishida, Zheng, and Akebata, aims to generate pure CO_2 from any oxidizable carbonaceous material[38]. In the conventional chemical looping system illustrated in Figure 8, two separate reactors are employed: one for fuel combustion and another for air, where the solid material, referred to as oxygen carriers, undergoes regeneration.

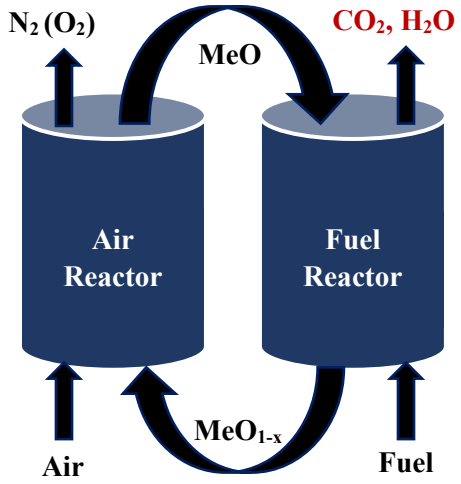

Figure 9. Chemical Looping Combustion (CLC) system.

This process involves the continuous oxidation and reduction of oxygen carriers (Equations (1) and (2), facilitating their circulation throughout the integrated CLC unit [39]. The resulting gas primarily comprises CO_2 and H_2O. Following water condensation and purification, a highly concentrated CO_2 stream, suitable for transportation and storage, is obtained[40].

$$(2n + m)Me_xO_{y-1} + (n + 0.5m)O_2 \rightarrow (2n + m)Me_xO_y \quad \textbf{R5.}$$

$$C_nH_{2m} + (2n + m)Me_xO_y \rightarrow nCO_2 + mH_2O + (2n + m)Me_xO_{y-1} \quad \textbf{R6.}$$

2.4.2 Chemical Looping Reforming

Since reforming methods have been around for decades and produce hydrogen at a lower cost than either solid fossil fuels or renewable energy sources, they have several benefits. To separate H_2 and CO_2 from the syngas produced in these reactors a process must be carried out. Despite the availability of CO_2 capture technology integrated with H_2 production, its high cost remains a significant barrier to widespread adoption[40]. Employing an oxygen carrier, reforming processes like steam reforming (SRM) and dry reforming (DRM) transform organic carbon into syngas mainly composed by CO and H_2 [41].

$$CH_4 + H_2O \leftrightarrow CO + 3H_2 \qquad \textbf{R7.}$$

$$CH_4 + CO_2 \leftrightarrow 2CO + 2H_2 \qquad \textbf{R8.}$$

These techniques usually involve the following steps: producing syngas at an elevated temperature using a high-temperature catalytic reformer; increasing the hydrogen content at an intermediate temperature using a water-gas shift unit; and removing carbon dioxide using a low-temperature separation process. However, for instance, the favored Ni-based catalyst frequently experiences deactivation because of active phase sintering, poising, or coke buildup. Chemical-looping reforming operates on the same fundamental principles as chemical-looping combustion, but with a focus on producing synthesis gas instead of heat. Unlike combustion, where complete oxidation to CO_2 and H_2O is desired, the aim here is to maintain a low air-to-fuel ratio to prevent full oxidation. In this process, a solid oxygen carrier serves as a source of pure oxygen, eliminating the need for costly and energy-intensive air separation. This approach facilitates the partial oxidation of hydrocarbon fuels, as illustrated in Figure 9[42].

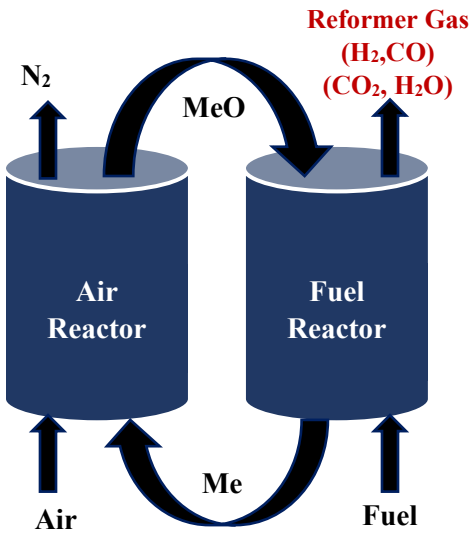

Figure 10. Chemical looping Reforming system.

2.4.3 Chemical Looping Gasification

Chemical looping gasification in figure 10 is a novel based on the concept of chemical looping combustion. However, a solid material, for example biomass or coal with gas assisted by an oxygen carrier that is combusted to produce high quality syngas therefore, mainly used for Fisher- Tropsch crude production instead of heat as the final product[43].

$$C_nH_{2m}O_p + (n-p)Me_xO_y \rightarrow nCO + mH_2 + (n-p)Me_xO_{y-1} \quad \textbf{R9.}$$

$$O_2 + 2Me_xO_{y-1} \rightarrow 2Me_xO_y \quad \textbf{R10.}$$

CLG employs a special material called an oxygen carrier. This oxygen carrier, typically a metal oxide, acts as a shuttle, transporting oxygen from air to the fuel reactor without ever mixing air and fuel directly. The oxygen carrier cycles between two states. Oxidized State the oxygen carrier readily captures oxygen from air in a separate reactor. Reduced State oxygen carrier then travels to the fuel reactor, where it transfers its oxygen to the fuel, undergoing reduction. The process is broken into two stages. Into the fuel reactor (equation 8) solid fuel is introduced. Here, it reacts with the oxygen carrier in its reduced state. This reaction produces syngas (hydrogen

and carbon monoxide) and reduces the oxygen carrier further. On the other hand, the air reactor (equation 9) the reduced oxygen carrier is then transported to the air reactor. In this reactor, it encounters air and readily captures fresh oxygen, regenerating itself and preparing for another cycle in the fuel reactor. Chemical looping gasification presents a compelling approach for cleaner and more efficient syngas production. Overcoming the current challenges and advancing research in oxygen carrier development, reactor design, and large-scale integration hold the key to unlocking the full potential of this transformative technology. As CLG matures, it has the potential to revolutionize the way we convert fuels into valuable syngas, paving the way for a more sustainable energy future [44].

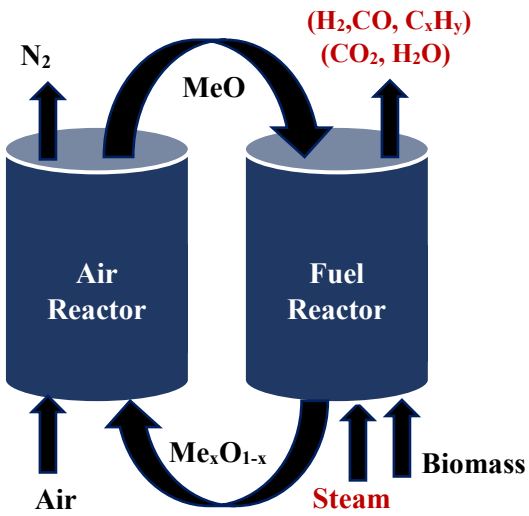

Figure 11. Chemical looping Gasification system.

2.4.4 Chemical Looping with Oxygen Uncoupling

Chemical looping with Oxygen Uncoupling (CLOU) in figure 12 employs a technique like chemical looping combustion but with a specific focus on oxygen production. Traditionally, oxygen is obtained through cryogenic, adsorption, or membrane air separation technologies. While these methods are well-established, they often entail high energy consumption and substantial capital investment, which may not align with the goals of energy-efficient economies[45]. In pursuit of more cost-effective and energy-saving alternatives for oxygen production, the concept of chemical looping air separation (CLAS) has been introduced.

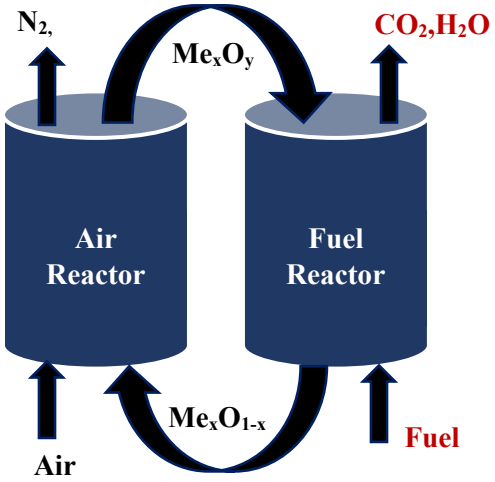

Figure 12. Chemical looping with Oxygen Uncoupling.

Similar to traditional combustion, this process involves the fuel combusting directly with the gaseous oxygen that is released from the oxygen carrier. To enable the fuel to burn later, the oxygen carrier first breaks down the oxidized form of the metal oxide, MeO_2 (reaction 10). This releases oxygen into the atmosphere. Next, for reoxidation, the depleted oxygen carrier is moved

to the air reactor (equation 11). Hence, when employing solid fuels like coal or biomass, gasification becomes necessary to facilitate their oxidation by a solid oxygen carrier. Another approach could involve utilizing an oxygen carrier with the ability to release oxygen in the gas phase under conditions found in the fuel reactor[46]. As an essential ingredient in many sectors of the economy, such as glass production, chemical synthesis, medicine, metallurgy, oxygen is currently the second most produced chemical by volume worldwide[35]. Unlike conventional CLC operations, Chemical Looping with Oxygen Uncoupling (CLOU) eliminates the direct connection between the oxygen carrier and the fuel gas[47].

$$Me_xO_{y-2}(s) + O_2(g) \rightarrow Me_xO_y(s) \quad \textbf{R11.}$$

$$Me_xO_y(s) \rightarrow Me_xO_y(s) + O_2(g) \quad \textbf{R12.}$$

2.4.5 Chemical Looping Dry Reforming (CLDR)

Chemical looping dry reforming (CLDR) in figure 13 is an innovative technology that employs CO_2-air as oxidizing agents, deviating from the conventional CLC process that relies on air alone. CLDR involves three key stages: CH_4 reduction, CO_2 reforming, and air oxidation [48]. Notably, the process yields high-purity H_2 or CO streams from the air reactor without requiring additional purification when utilizing H_2O and CO_2 as oxidants[36]. It includes multiple crucial steps in the CLDR process. In a reducing environment, like methane CH_4, an oxygen carrier (MeO) is first reduced to its metallic state (Me). The reduced oxygen carrier (Me) then recovers most of its lattice oxygen to move to an intermediate state, and in a weakly oxidative environment (CO_2), CO_2 is also reduced to CO. After recovering the remaining lattice oxygen, the intermediate state oxygen carrier (MeO_{1-x}) finally oxidizes by air to return to its starting state (MeO). The oxygen carrier flows throughout the process, acting as a continuous reducing

medium for CO_2 reduction as well as an oxidizing medium for fuel conversion. This makes it possible for the CLDR process to efficiently use an inexpensive source of oxygen[49]. While methane is commonly used as the fuel in CLDR, the process aims to optimize CO_2 activation rather than maximizing synthesis gas yield as in traditional methane dry reforming. CLDR can accommodate various fuels, provided the oxygen carrier exhibits sufficient reactivity with them. Notably, a low concentration CO_2 stream is processed in the second step of the CLDR process, whereas a high concentration, or even pure, CO_2 stream is produced in the first. Consequently, CLDR offers intrinsic CO_2 separation and effective CO_2 activation with low energy requirements and low costs, making it an attractive and promising technology to replace traditional combustion or CO_2 reforming processes.

Main equations of the process:

$$Dry\ Reforming: CH_4 + CO_2 \rightarrow 2CO + 2H_2 \quad \textbf{R13.}$$

$$Oxidizer: Me + CO_2 \rightarrow MeO + CO \quad \textbf{R14.}$$

$$Reducer: CH_4 + MeO \rightarrow CO + 2H_2 + Me \quad \textbf{R15.}$$

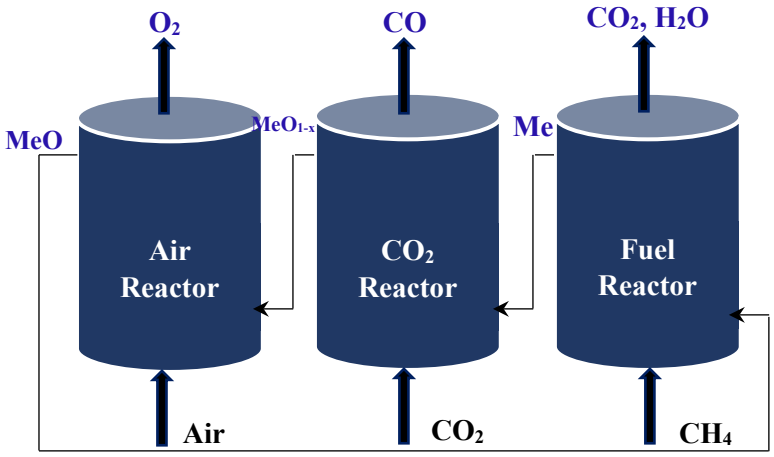

Figure 13. Chemical looping of Dry Reforming of methane.

2.5 Perovskites

Perovskites have been around for over a century, named after Lev Perovski, a Russian mineralogist who first identified a specific mineral with this structure in 1792[50]. However, in recent years, there's been a surge of interest in a special type: organic-inorganic perovskites. This novel family of materials known as Organic-Inorganic Hybrid Perovskites (OIHPs) combines the benefits of inorganic and organic semiconductors to provide several advantages. High performance strong optical, electrical, and magnetic characteristics of inorganic semiconductors are carried over to OIHPs, which makes it easier to create high-performance devices with better functionality. Simple fabrication: OIHPs can be produced more affordably and with less complexity than traditional inorganic semiconductors by employing methods like solution processing at comparatively low temperatures. This simplicity of manufacturing lowers production costs and improves scalability. Versatility OIHPs are remarkably chemically flexible and compatible due to the integration of organic components into their structure. This makes them appropriate for a wide range of applications across many sectors. Their adaptability makes it possible to innovate in fields like energy conversion, photonics, and electronics[51]. Perovskites and perovskite-derived structures are esteemed for their exceptional stability and remarkable ability to incorporate different positively charged atoms (cations) making them incredibly versatile. This class of materials exhibits a simple formula (ABX_3) where A and B are known as cations and X the anion that forms bonds with cations as shown in figure 14. Divalent base alkaline, alkaline-earth, or rare-earth metal elements with greater ionic radii usually occupy the A-site in the perovskite lattice. In contrast, elements of transition metals with smaller ionic radii dominate the B-site. In terms of the X position, bigger ions like halides, sulfides, and nitrides as well as oxygen frequently occupy it. In particular, the atoms in position 'A' are larger than those in position 'B', and both sites are

interchangeable with different metals or semimetals from the periodic table[52]. The potential applications of these versatile materials are vast. Perovskite solar cells[53] are a hot topic in the renewable energy sector. Their ability to efficiently convert sunlight into electricity has researchers excited about the possibility of creating cheaper and more efficient solar panels. Perovskites hold promise for next-generation LEDs[54]. Their tunable light emission properties could lead to brighter, more efficient displays and lighting solutions. The potential applications extend far beyond light-related technologies. Perovskites are being explored for use in sensors, catalysts, and even next-generation memory devices. Perovskite research is a rapidly evolving field. While challenges remain, such as long-term stability and large-scale manufacturing, the potential of these materials is undeniable. As scientists continue to unlock their secrets, perovskites could play a significant role in shaping the future of technology and sustainability.

Perovskite catalysts have favorable effects. This material's generic formula is ABX_3, where B is typically a transition metal (Fe, Ni, Cu, Co, etc.) and A is typically an alkaline earth metal (Be, Mg, Ca, Ba, etc.). These metals make good candidate catalysts because of their tunable catalytic performances, good redox properties, and thermochemical stability[55]. Owing to its excellent mechanical qualities, high thermal stability, and respectable activity, perovskite-type oxides are utilized in the production of a variety of high temperature electrochemical devices, as well as serving as a catalyst for redox reactions and an oxygen carrier in the CLR and CLC processes [56]. Perovskite compounds can be formed by about 90% of the metals in the periodic table [57] and easily tune the catalytic, electronic and structural characteristics. Moreover, perovskites often exhibit notable catalytic activity due to their unique crystal structures, facilitating redox processes and the exchange of oxygen atoms. Their reactivity enables these materials to effectively drive chemical transformations. On this study the focus is on the production of syngas by using the

chemical looping technology that in advantage of others will result in a maximum yield of gas with the assistance of dual phase catalyst.

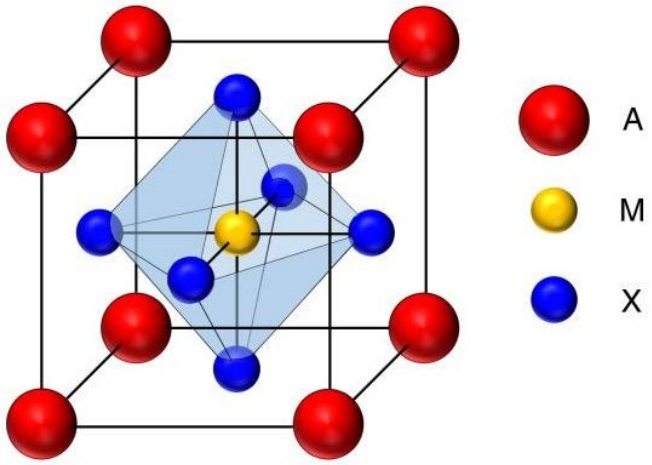

Figure 14. Crystal structure of Perovskites.

The thermochemical conversion methods of biomass include combustion, liquefaction, pyrolysis, and gasification[58] . For instance, steam biomass gasification is a promising approach to producing hydrogen-rich syngas for its capacity to increase the heating value of the produced syngas by means of quick conversion kinetics. However, through this method it is observed low amounts of hydrogen and significant amounts of tar during gasification, which prevents its large-scale implementation[59]. In addressing these challenges, has become a key component of the gasification process in tackling these issues. It mitigates tar formation, accelerates the conversion of biomass, and improves both the quantity and quality of syngas generated. In Chen F. et al.'s studies, the employment of Ni/CaAlOx resulted in a notable enhancement of H_2 yield, increasing from 18vol% to 45vol% [59]. Similarly, in Moghadam RA. et al.'s study, the utilization of $CaMg(CO_3)_2$ yielded 485.9g.kg-1 of syngas, with 83.3g.kg-1 of H_2 produced. The presence of catalysts during this thermochemical process facilitated secondary reactions such as water gas

shift, tar cracking, and hydrocarbon reforming. Several types of catalysts have been explored to mitigate tar content, while simultaneously boosting syngas production and enhancing its quality. Transitional methods catalysts as Fe-based[60], Ni-based[61], and Co-based[62] have been studied to lower tar production in biomass thermochemical conversion. However, this catalyst type presents lack stability due to coke deposition sintering and agglomeration. In addition, noble metal catalysts are also very helpful, but their costs are unbearable in their industrial applications. Furthermore, even though noble metal catalysts are very advantageous their high cost makes them unsuitable for its application.

2.6 Perovskite Synthesis

Perovskites have emerged as a revolutionary class of materials with the potential to transform various fields like solar energy, electronics, and catalysis. Their unique properties stem from their versatile structure, typically represented by the formula ABO_3, where A and B can be cations of different elements. This flexibility allows for a vast array of compositions, each with the potential to exhibit remarkable characteristics. Perovskite synthesis is a crucial step in unlocking the potential of these materials. By carefully selecting precursors and tailoring the synthesis process, scientists can create perovskites with specific properties optimized for desired applications.

Perovskite synthesis methods have indeed undergone significant advancements since their initial development via the simple ceramic method in the 1970s. The primary focus of these studies has been to enhance the physical properties of perovskite materials, which are crucial for catalytic applications where surface area plays a pivotal role[63]. Consequently, various more efficient synthesis routes have emerged, including the sol-gel method, solid-state reaction, Pechini and modified Pechini techniques, wet impregnation method, and spray drying method (Fig. 15).

Perovskites made with these techniques have been used by researchers in a variety of CL technology applications.

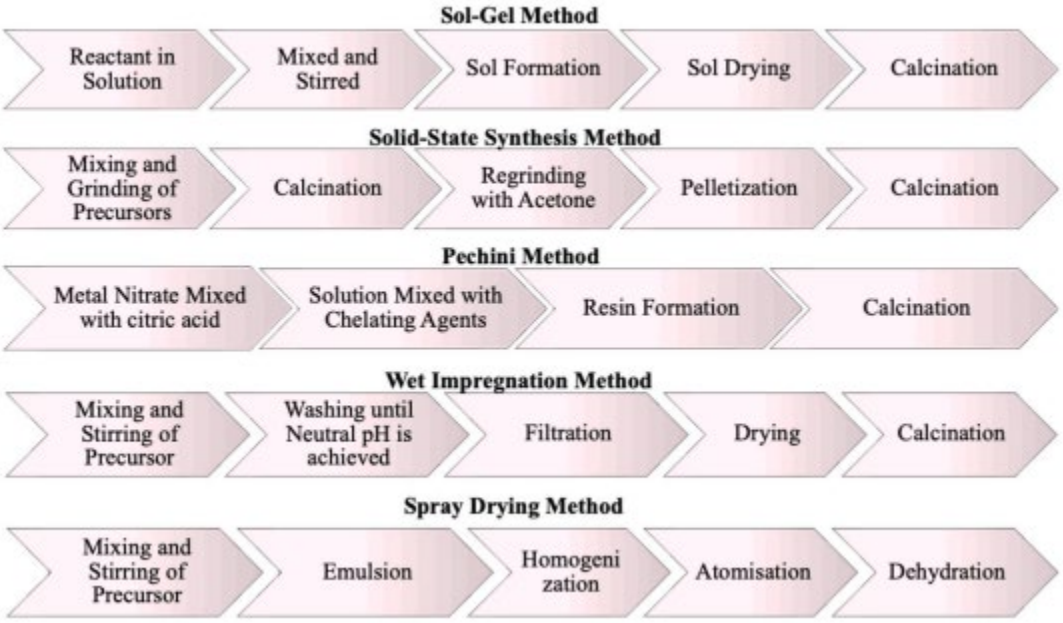

Figure 15. Perovskites Synthesis methods.

3 Chapter: Methodology

3.1 Materials

The focus of this work is on analyzing the catalytic pyrolysis and gasification tests by using Biomass-Recycled Railroad Ties (RRT) provided by a local company in Oklahoma City. To prepare the RRT for experimentation, it underwent a series of steps in figure 15: initially it was dried at 110 ℃ for 16 hours then it was grounded and sieved at the desired particle size of 120 to 130 µm.

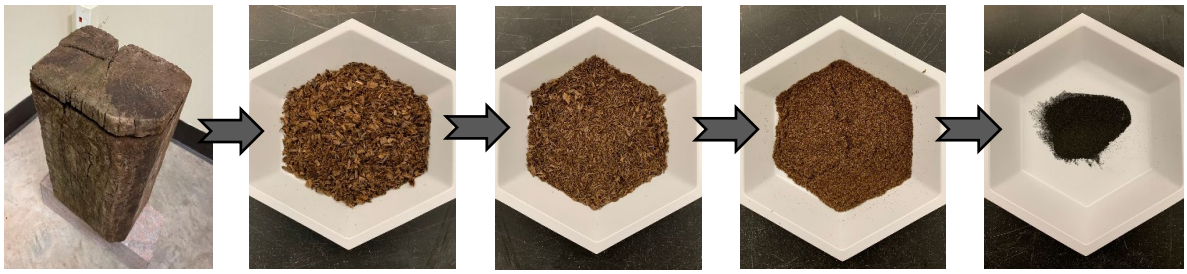

Figure 16. Railroad tie pretreatment. a) Railroad ties biomass, b) sized down RRT, c) dried and grounded, d) sieved biomass to particles size bellow µm 300, e) produced biochar (sieved for the second time to achieve the desired particle size) for other use proposes.

On table 1 is presented the proximate and ultimate analyses of the RRT biomass. The RRT biomass composition includes 61.3% carbon (C), 6.6% hydrogen (H), and 28.8% oxygen (O). Consequently, the molar ratios of hydrogen to carbon (H/C) and oxygen to carbon (O/C) are 1.292 and 0.352, respectively. These ratios suggest that the molecular formula of the RRT biomass is defined as $CH_{1.292}O_{0.352}$.

Table 1. Proximate analysis and ultimate analysis of the recycled Railroad ties.

Proximate values (% weight)	***Railroad ties***
Volatile	90.9
Fixed Carbon	18.9
Ash	0.40
Ultimate values (%weight)	***Railroad ties***
Hydrogen	6.6
Carbon	61.3
Nitrogen	0.4
Oxygen	28.8
Sulfur	0.1

3.2 Dual-phase catalyst synthesis

On this study the assisted citric acid Pechini method [64] shown in figure 16 is used to prepare the dual phase catalysts $Ca_2Fe_2O_5$, $CaFe_2O_5$+$CuFe_2O_4$, $CaFe_2O_5$+$CoFe_2O_4$, and $CaFe_2O_5$+$NiFe_2O_4$. In this process Ca $(NO_3)_2 \cdot 4H_2O$), Fe $(NO_3)_3 \cdot 9H_2O$ and citric acid were mixed according to the desired molar ratios (Ca: Fe: citric acid = 2:2:4 for $Ca_2Fe_2O_5$). As for the other phases $CaFe_2O_4$, $CuFe_2O_4$, $CoFe_2O_4$, and $NiFe_2O_4$ and the desired molar ratios (M: Fe: citric acid = 1:2:6 as M stands for the metals). The mixture was dissolved in deionized water and stirred constantly for 2h at 80°C separately (base phase and second phase). After, it was added to each sample ethylene glycol ($C_8H_{18}O_5$) with the molar ratio of 4 for the base phase and 6 for the second phase and mixed for 8h at 80°C. With the base phase still on the hot plate the second phase was slowly added into the base phase by a pipette after that placed into crucibles as one solution and dried at 180°C for 12h then calcinated in air in a muffle furnace at 850°C for 4h, temperature ramp 5°C/ min.

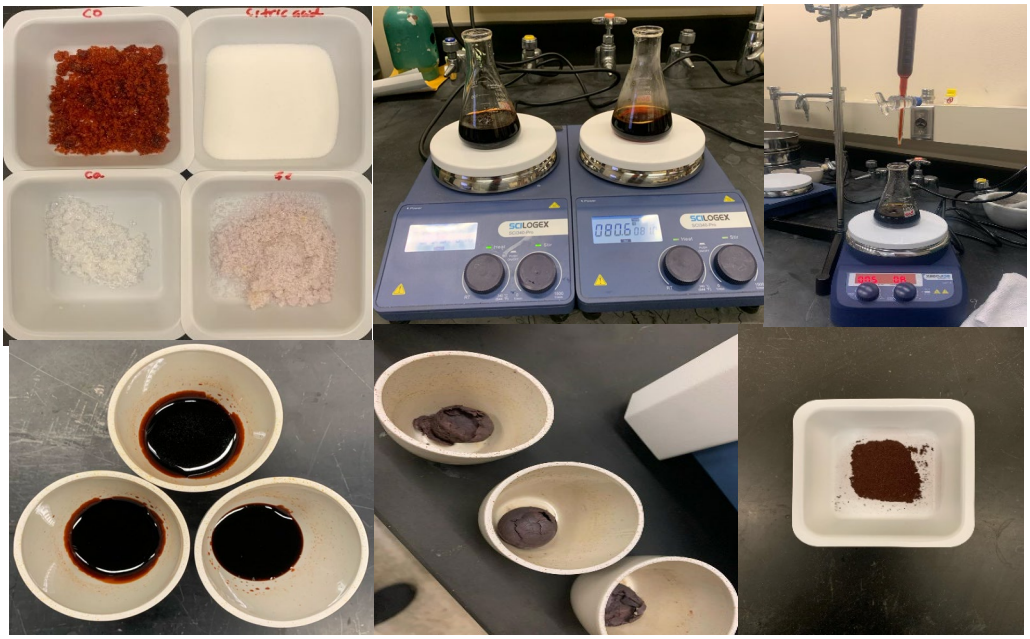

Figure 17. Pechini synthesis.

3.3 Set up and Procedure.

A fixed bed reactor was used for the RRT pyrolysis steam gasification with dual phase catalyst process as seen in figure 17. The setup included an electrical furnace, a reactor, a temperature controller furnace, a syringe pump, a gas wash bottle, gas bags, and flow meters. The quartz tube reactor utilized in the study has an outside diameter of 0.75", an inner diameter of 0.5", and a length of 40". The experiment involved feeding the reactor with 4g ± 0.05g of RRT biomass mixed by stirring for 5 min 0.4g ± 0.05g the dual phase catalyst. After that the mixture was loaded into the quartz tube reactor. N_2 was prior purged into the reactor to provide an inert atmosphere for 3 min. The desired tests temperatures were 650°C, 750°C, and 850°C at the heating rate of 20°C/min and N_2 flow rate of 50ml/min. Water was injected at the desired flow rate 0.1ml/min before reaching the desired temperature due to the production of the gas even before the desired temperature by a syringe pump. The produced gas was first cleaned and dried in a gas wash bottle and then collected in Tedlar® bags for every 10 minutes (the setup is depicted on figure 18).

Table 2 shows the properties of Shimadzu 2014 (GC) that was used to measure the concentrations of the syngas of H_2, CO, CH_4, and CO_2. It consists of a Shin Carbon column of 2.0 m length , 0.53 mm inner diameter, 212.00 µm of film thickness where the carrier gas is argon (Ar). The Thermal conductivity detector (DTCD) temperature was 100℃ with 70mA of current.

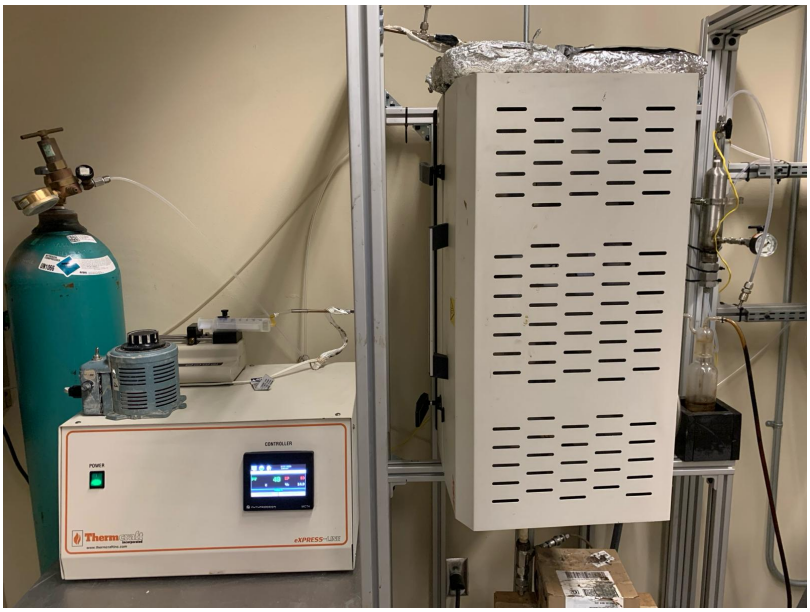

Figure 18. Fixed bed for pyrolysis and gasification processes.

Table 2. GC Shimadzu 2014 configuration.

Shimadzu 2014 (GC)	
Column temperature (℃)	40
Pressure (Kpa)	278.5
Linear velocity (cm/s)	187.9
Purge flow (mL/min)	3
Total flow (mL/min)	10.5
Injection mode	split
Split ratio	2

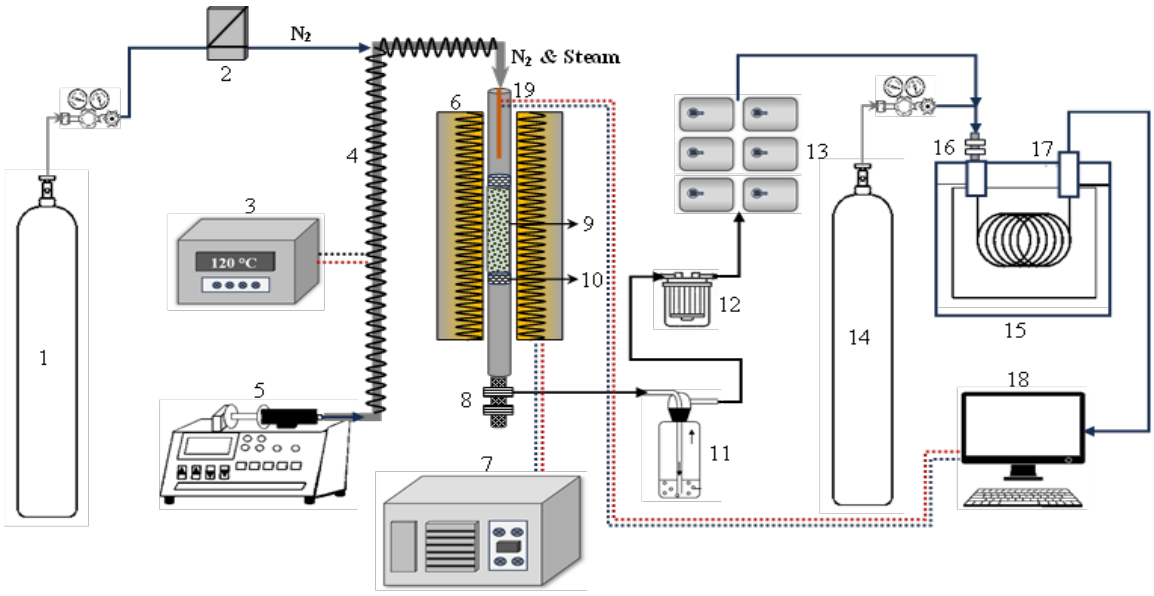

Figure 19. Schematic diagram of fixed bed catalytic biomass refinery system. (1) N_2 cylinder; (3) heating tape temperature controller; (4) Heating tape; (5) HPLC syringe pump 0.1 – 10 ml/min; (6) fixed bed furnace and quartz tubular reactor; (7) temperature controller of furnace; (8) bio-oil collector; (9) biomass sample; (10) sample stopper- quartz wool; (11) gas wash bottle; (12) membrane filter; (13) gas bags; (14) Argon cylinder; (15) Gas chromatograph, Shimadzu; (16) split/spitless injection port; (17) Thermal conductivity detector; (18) Computer with Lab solution software; (19) online thermal sensor.

3.4 Data evaluation

The volume of syngas gas of each component (H_2, CO, CO_2, CH_4) were calculated as follows:

$$V_{H_2} = C_{H_{2GC}} \times V \quad \textbf{16.}$$

$$V_{CO} = C_{CO_{GC}} \times V \quad \textbf{17.}$$

$$V_{CH_4} = C_{CH_{4GC}} \times V \quad \textbf{18.}$$

$$V_{CO_2} = C_{CO_{2GC}} \times V \quad \textbf{19.}$$

Where V is the gas volume collected in a sample bag every 10 minutes, C_{CO}, C_{H2}, C_{CO2}, and C_{CH4} is the syngas gas concentration of CO_2 given by the GC. The yield of each gas component was computed as follows:

$$Y_i = \frac{V}{m} c_i \qquad \textbf{20.}$$

Where V was the total gas volume collected in the sample bag, c_i was the actual concentration of each gas component $_i$ and m that represents the RRT biomass. The total gas component yield is the sum of hydrogen gained in every 10 min:

$$Y_{sum,H_{2,out}} = \sum_{1}^{n} Y_{i,H_{2,out}} (n = 1, 2, 3, 4, 5, 6) \qquad 21.$$

Where $Y_{i,H2,out}$ represents the H_2 yield accumulated with number *i* gas bag and $Y_{sum,H2,out}$ denotes the total hydrogen yield. Carbon conversion efficiency was used to evaluate to investigate biomass conversion in thermal reactions:

$$Carbon\ conversion = \frac{12}{22.4 C_b}\left(Y_{CO} + Y_{CO_2} + Y_{CH_4}\right) \times 100\% \qquad \textbf{22.}$$

Where C_b is the carbon content of biomass. Furthermore, the molar ratio , CO/CO_2 and H_2/CO molar ratio:

$$\frac{H_2}{CO} molar\ ratio = \frac{Moles\ of\ H_2\ product}{Moles\ of\ CO\ product}$$

$$\frac{CO}{CO_2} molar\ ratio = \frac{Moles\ of\ H_2\ product}{Moles\ of\ CO\ product}$$

3.5 Catalyst Characterization

The crystalline of OCs were observed by X-ray diffraction (XRD) which was conducted by Rigaku Smalab X-ray Diffractometer using a Cu K a radiation (2 = 0.15046 nm), a target current of 40 mA, and a target voltage of 40 kV. The diffraction angle 20 was scanned from 20 to 80 ° with a step of 0.0167 °/s. Transmission Electron Microscopy (TEM) was conducted using the JEOL 2010F Field Emission Transmission Electron Microscope to view ~3-5 clusters of each catalyst type. For morphological analysis, the scanning electron microscopy (SEM) and energy dispersive spectrometer (EDS) were conducted using the Thermo Quattro S field-emission environmental Scanning Electron Microscope.

4 Chapter 2: Results and Discussions

4.1 SEM-EDS

ThermoFisher Quattro S with an acceleration voltage of 30 kV was used to conduct analysis utilizing Energy Dispersive Spectrometer (EDS) in conjunction with scanning electron microscopy (SEM). The mapping images of the different catalysts used in the gasification process, such as $Ca_2Fe_2O_5$, $Ca_2Fe_2O_5$+$CuFe_2O_4$, $Ca_2Fe_2O_5$+$CoFe_2O_4$, and $Ca_2Fe_2O_5$+$NiFe_2O_4$, are shown in Figure 21. The EDS images show that the catalyst $Ca_2Fe_2O_5$+$CuFe_2O_4$ stands out for having the most uniform distribution of its constituent elements, Fe, Ca, and Cu. In addition, the SEM shows a densely packed particle structure on the same catalyst confirming the uniform distribution of its components. On the other hand, the $Ca_2Fe_2O_5$ catalyst shows a good distribution only for the Ca and Fe components leaving a non-uniform distribution for O_2. This is consistent with the other catalysts, where only one/two components show acceptable dispersion. It is crucial to emphasize that improved catalyst performance is correlated with a greater degree of component distribution[65]. The results of EDS mapping are shown in table 3. Confirming a uniform distribution with all catalysts.

Weight%				
Element	**$CaFe_2O_5$**	**$CaFe_2O5$+CuFe2O4**	**CaFe2O5+CoFe2O4**	**CaFe2O5+NiFe2O4**
Fe	45.379	49.335	45.537	37.068
O	29.046	22.517	30.138	32.037
Ca	20.278	11.541	11.164	12.992
Cu	-	11.879	-	-
Co	-	-	3.876	-
Ni	-	-		6.055

Table 3. The extracted spectrum weight % for each OC element.

4.2 TEM

The JEOL 2010F electron microscope was utilized to examine approximately 3-5 clusters of each catalyst type. SEM-EDS analysis revealed a favorable dispersion of components within the $Ca_2Fe_2O_5$+CuFe2O4 catalyst. TEM-EDS imaging depicted an almost spherical structure for the referred catalyst with uniform dispersion of its constituents. Micrograph analysis confirmed the richness of Cu, Fe, and Ca elements in the $Ca_2Fe_2O_5$+CuFe2O4 catalyst through observed peaks. Conversely, the $Ca_2Fe_2O_5$+NiFe2O4 catalyst exhibited a more irregular spherical shape, with peaks indicating the presence of its primary components. Additionally, XRD findings for both catalysts corresponded to these structural compositions.

4.3 XRD

The Rigaku SmartLab X-ray diffractometer was used to conduct the XRD tests on the five catalysts samples. On figure 20 the XRD results for the unreacted catalyst. It is observed that all the crystals phase of the $Ca_2Fe_2O_5$ are present on the dual phases catalysts as crystalized on the catalyst base.

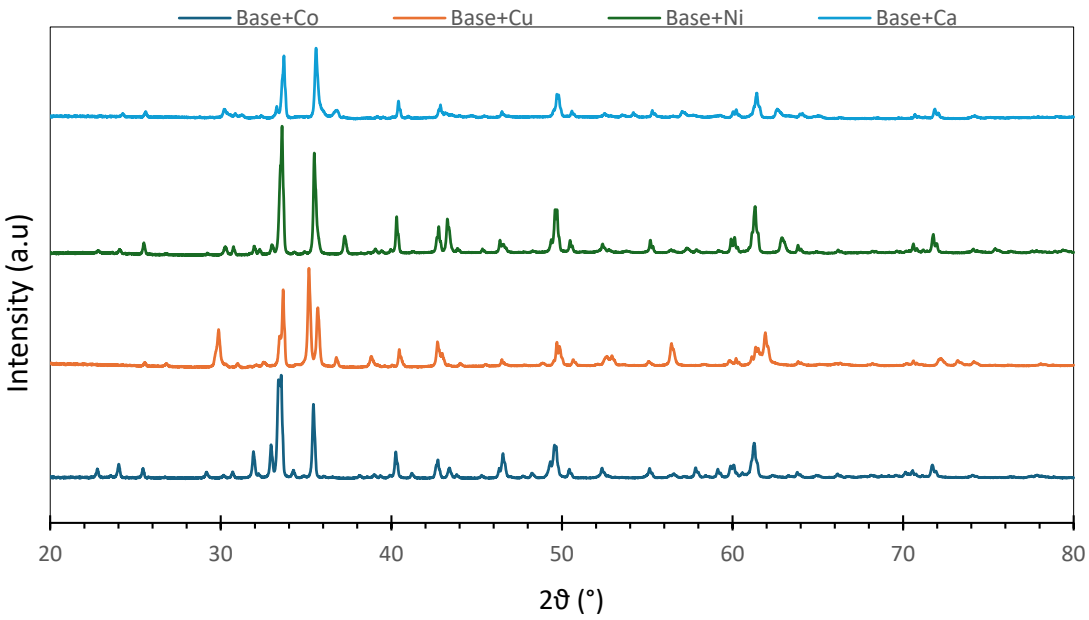

Figure 20. XRD of unreacted and reacted catalyst.

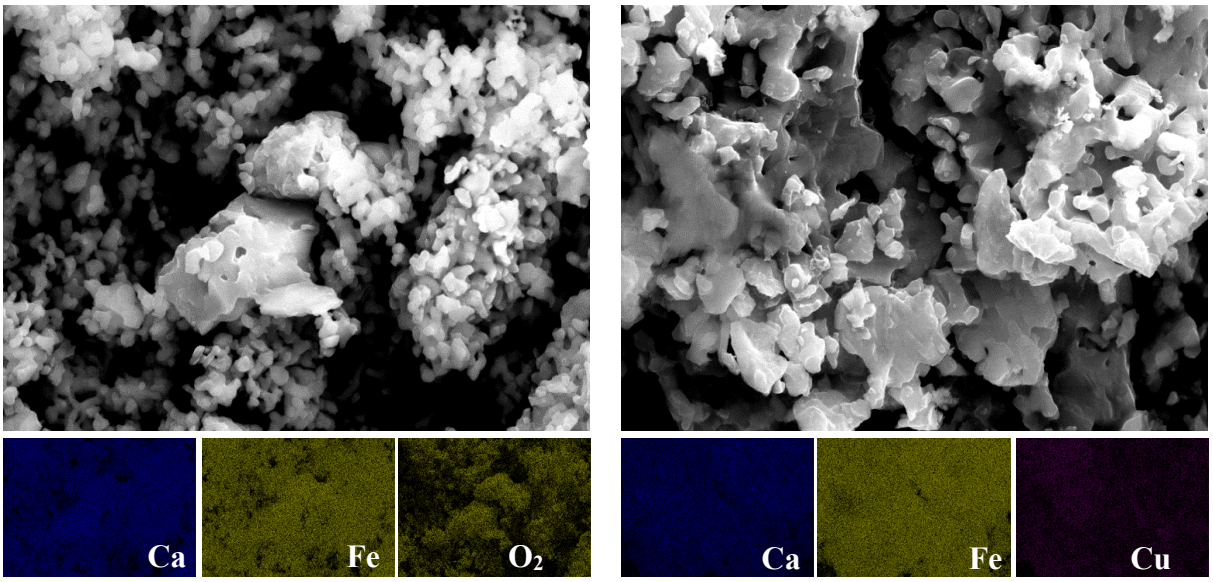

(a)

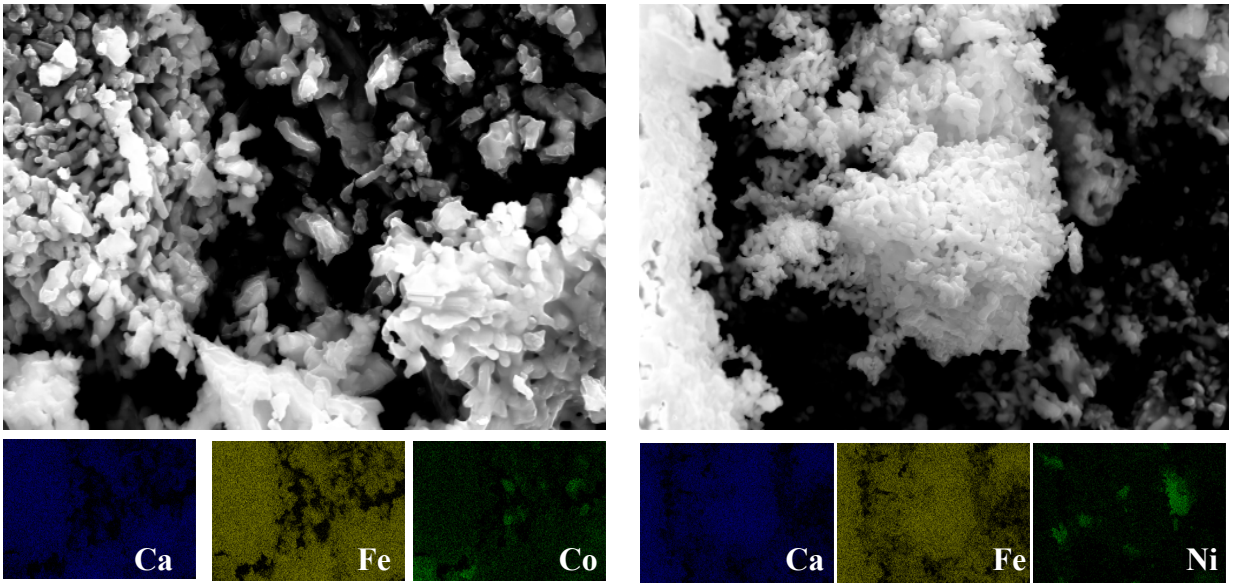

(c)

Figure 21. SEM-EDS images of a) $Ca_2Fe_2O_5$, b) $Ca_2Fe_2O_5$+$CuFe_2O_4$, c) $Ca_2Fe_2O_5$+$CoFe_2O_4$, and d) $Ca_2Fe_2O_5$+$NiFe_2O_4$ catalysts.

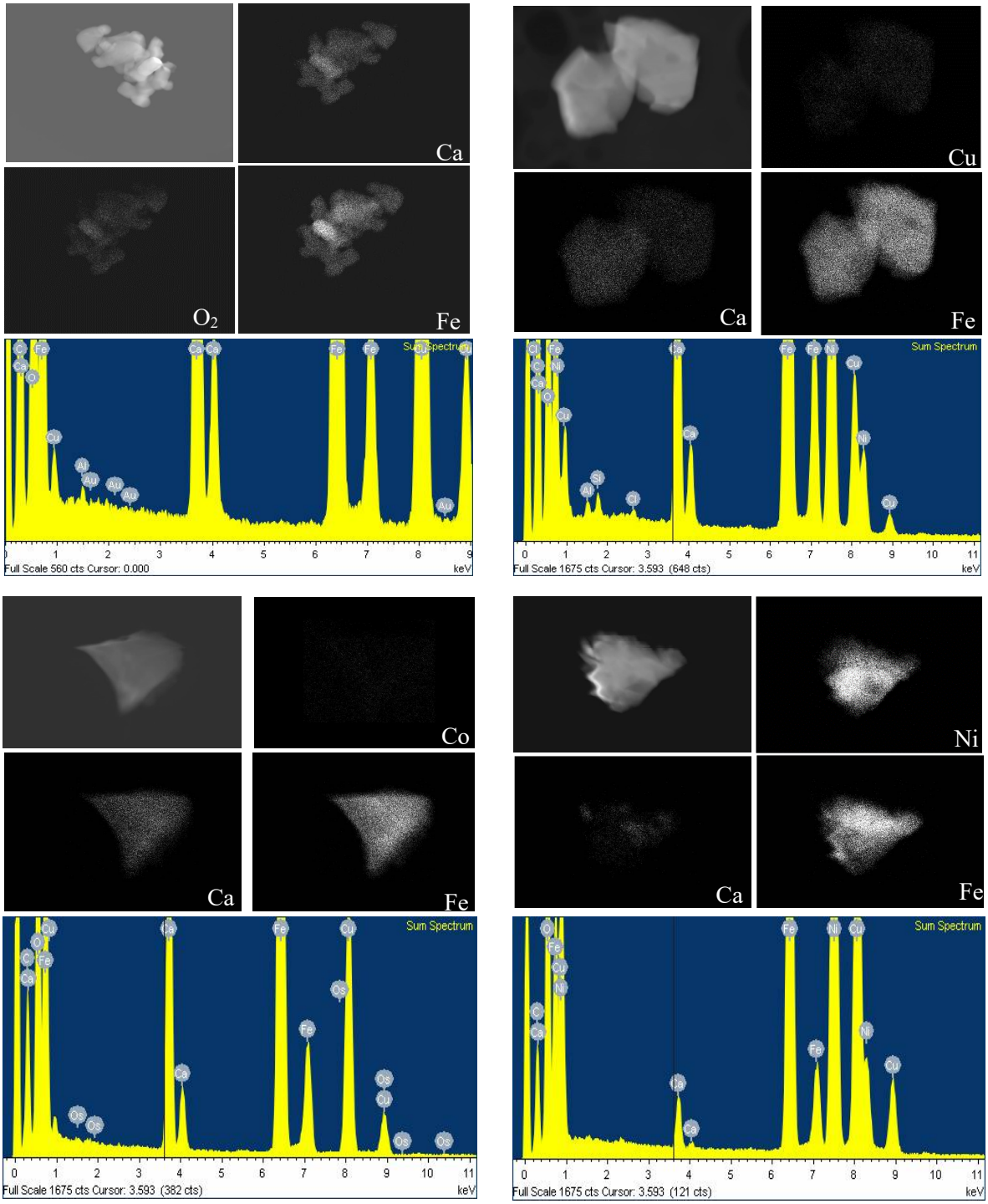

Figure 22. TEM images of a) $CaFe_2O_5$, b) $CaFe_2O5$+$CuFe_2O_4$, c) $CaFe2O_5$+$CoFe_2O_4$, and d) $CaFe_2O_5$+$NiFe_2O_4$ catalysts.

4.4 CLG without gasifying agent

Pyrolysis occurs first at 650-850℃. On the first stage RRT undergoes into decomposition. The cellulosic, hemicellulose and the lignin components start breaking their bonds. Then the volatiles matters are released tar, CO, CH_4, H_2, CO_2 and char (R23) [66]. The oxygen carrier reacts with the volatile matter in a redox reaction to increase the yield of syngas while decreasing the char and tar.

Figure 23 shows the effects of pure pyrolysis in comparison to catalytic pyrolysis when the oxygen carrier is introduced. The yield of each component of syngas is shown throughout the pyrolysis phase using pure railroad ties biomass and with the application of four catalysts ($Ca_2Fe_2O_5$, $Ca_2Fe_2O_5$+$CuFe_2O_4$, $Ca_2Fe_2O_5$+$CoFe_2O_4$, and $Ca_2Fe_2O_5$+$NiFe_2O_4$), categorized by different temperatures in the experiment. Clearly, hydrogen (H_2) demonstrates a notably high production when generated via $Ca_2Fe_2O_5$. The concentrations of H_2 increase with rising temperatures, attributed to secondary reactions occurring at higher temperatures[67]. Among the catalysts, $Ca_2Fe_2O_5$ is the most efficient, exhibiting the highest yield of H_2 at elevated temperatures 5.68mol.kg^{-1} and 5.94mol.kg^{-1} compared to the pure RRT 4.17mol.kg^{-1} and 3.96mol.kg^{-1} at 750°C and 850°C respectively. Furthermore, the reactions at low temperature 650°C didn't have much significance, a gradual decrease in the amount of H_2 is observed, suggesting that the catalysts had a minimal impact on H_2 yield at the lowest temperature. As for the rest of the dual phase OC's it didn't have much impact on the yield of hydrogen. In Figure 23b, the yield of CO is shown. It is evident that the same pattern is observed. High yield of CO at highest temperatures suggesting that it could be generated through partial oxidation and methane decomposition reactions (26, 27). four catalysts contribute to an increase in CO yield during the pyrolysis phase compared to pure railroad ties biomass pyrolysis. Moreover, at 750°C, the $Ca_2Fe_2O_5$ catalyst exhibits the highest CO yield, a

significant constituent of syngas. Furthermore, it is apparent that the impact of $Ca_2Fe_2O_5$ and $Ca_2Fe_2O_5$+CuFe2O4 is most notable at a higher temperature of 750°c. Furthermore, in figure 10c and 10d highlights the CH_4 and CO_2 yields. Normally, they are the very first compounds to decompose from the biomass; because of the high yields it is correct to affirm that this biomass was well decomposed that for further tests with gasification H_2 and CO will show higher yields in comparison with pyrolysis. The oxygen carrier has two main effects on this pyrolysis: act as cracking material when reacts with the char and tar matter it increases the yield of syngas. Lastly, the OC can present a selective characteristic to the O_2 donation reaction with the gases present on the pyrolysis reactor. Due to the availability of CH_4 that was partial oxidated when $Ca_2Fe_2O_5$ donates O_2 resulting in CO. Therefore, partial oxidation activity of $Ca_2Fe_2O_5$ presents a selectivity of CO.

Lastly, figure 22d illustrates the production of carbon dioxide (CO_2). The application of catalysts demonstrates a favorable impact on reducing CO_2 production. The amount of CO_2 present rises with temperature when pure railroad tie biomass is pyrolyzed. However, the use of catalysts is observed to mitigate this increase in CO_2 production. Overall, the catalysts exhibit selectivity towards other syngas components. Despite the minimal impact on H_2 yield, the catalysts contribute to increased yield of CO, potentially offering value for applications requiring specific CO/H2 ratios in syngas. Although with a limited effect of the catalyst on H_2 yield, it remains the most abundant component during the pyrolysis phase across different temperature levels. In addition, $Ca_2Fe_2O_5$+$CoFe_2O_4$ was the dual phase OC that produced more H_2, 5.08 $mol.kg^{-1}$ at 850℃.

The efficiency of catalytic biomass pyrolysis is heavily influenced by reaction temperature, as it facilitates further secondary crack reactions[68]. Lower temperatures, between 300-450°C, are generally more conducive to char yield, and medium temperatures between 450-600°C are more

favorable for bio-oil yield. On the other hand, temperatures beyond 600°C usually result in increased gas results[69]. The catalytic pyrolysis test was studied under different temperatures 650°C, 750°C, and 850°C. On figure 23, the trend of total gas yield with the respective concentrations of each syngas components with increasement of temperature during biomass pyrolysis, with and without the presence of the OC is demonstrated. It is observed that an increment in total gas production from 650°C to 850 °C. The interaction of multiple reactions involving the OC, biochar, tar, and syngas is responsible for the observed change in syngas concentration and yield. Although, it is supported the idea that during biomass pyrolysis, syngas generation generally increases with temperature, it's crucial to emphasize that greater temperatures can also increase the OC's ability to produce syngas.

The concentrations of syngas components fluctuate across different temperatures for both pure railroad ties (RRT) pyrolysis and the four OCs, as depicted in Figure 24. The concentrations of H_2 and CO increase gradually with the increment of the temperature. Due to several reactions supported by the high temperature CO_2 reforming along with Boudouard reactions and methane decomposition can take place. At 650 ℃, the concentration of H_2 of pure RRT pyrolysis is high than the ones observed with the presence of the catalyst. Meaning that the catalyst didn't have much impact at this temperature. While the dual-phase catalysts exhibit minimal impact on H_2 concentrations at 650℃ during the pure RRT pyrolysis, their reactivity is significantly enhanced at higher temperatures 850℃ with $Ca_2Fe_2O_5$ exhibiting best results [70]. The increase in CO and H_2 concentrations is attributed to the concurrent decrease in CH_4, promoted by catalyst addition and temperature elevation. CH_4 decomposition contributes to higher H_2 concentrations, while tar cracking releases CO_2, facilitating CO_2 reforming with CH_4 and Boudouard reactions, particularly at elevated temperatures, as described in the equations below [71]. Moreover, the partial oxidation

of CH_4 by O_2 molecules, facilitated by the catalyst, is suggested to further enhance CO and H_2 concentrations [72]. During pyrolysis the catalyst is reduced with the presence of the gases in the reactor CO, H_2, and CH_4 producing H_2O, Fe, and CO_2 (R31, R32,and R33). In summary, the observed trends underscore the intricate interplay between temperature, catalyst activity, and reaction pathways, influencing syngas composition. Furthermore, the OC $Ca_2Fe_2O_5$ shows CO selectivity, shifting from 26.08% with pure RRT to 39.82% with $Ca_2Fe_2O_5$. Furthermore, the temperature is important in this process: allows several reactions to happen, and in contrast Higher temperatures can enhance the OC's reactivity towards syngas but may lead to its sintering, compromising its effectiveness.

Biomass Pyrolysis: $CH_{1.292}O_{0.352} \rightarrow H_2 + CO + CO_2 + CH_4 + C_2 + \ldots + Tar + Char$ **R 23.**

Tar cracking: $C_nH_m \rightarrow {}^{m}/_{2}\, H_2 + C_n$ **R24.**

Tar cracking with CO_2: $\mathrm{C_nH_m(tar) + nCO_2 \rightarrow nCO + {}^{m}/_{2}\, H_2}$ **R25.**

Tar cracking with H_2O: $\mathrm{C_nH_m(tar) + nH_2O \rightarrow nCO + ({}^{m}/_{2} + n)H_2}$ **R25.**

CO_2 Reforming: $C_nH_m + nCO_2 \rightarrow 2nCO + {}^{m}/_{2}\, H_2$ **R26.**

Boudouard reaction: $C + CO_2 \rightarrow 2CO$ **R27.**

Partial Oxidation: $CH_4 + {}^{1}/_{2}\, O_2 \rightarrow CO + 2H_2$ **R29.**

Methane decomposition: $CH_4 \rightarrow C + 2H_2$ **R30.**

$Ca_2Fe_2O_5$ reduction with CO: $\mathrm{Ca_2Fe_2O_5 + 3CO \rightarrow 2CaO + 2Fe + 3CO_2}$ **R31.**

$Ca_2Fe_2O_5$ reduction with H_2: $\mathrm{Ca_2Fe_2O_5 + 3H_2 \rightarrow 2CaO + 2Fe + 3H_2O}$ **R32.**

$Ca_2Fe_2O_5$ reduction with CH_4: $\mathrm{4Ca_2Fe_2O_5 + 3CH_4 \rightarrow 8CaO + 8Fe + 3CO_2 + 6H_2O}$ **R33.**

Finally, figure 24 shows that H_2 occurs in the almost very beginning of the process within the 30min. In addition, only pure hydrogen is observed at the end of the process although it decreases gradually. Because of the consumption of the other components only pure hydrogen is seen in lower amounts. Furthermore, it suggests that water injection could make a huge difference in the early start of the process. Therefore, in gasification process steam will be injected at 100℃.

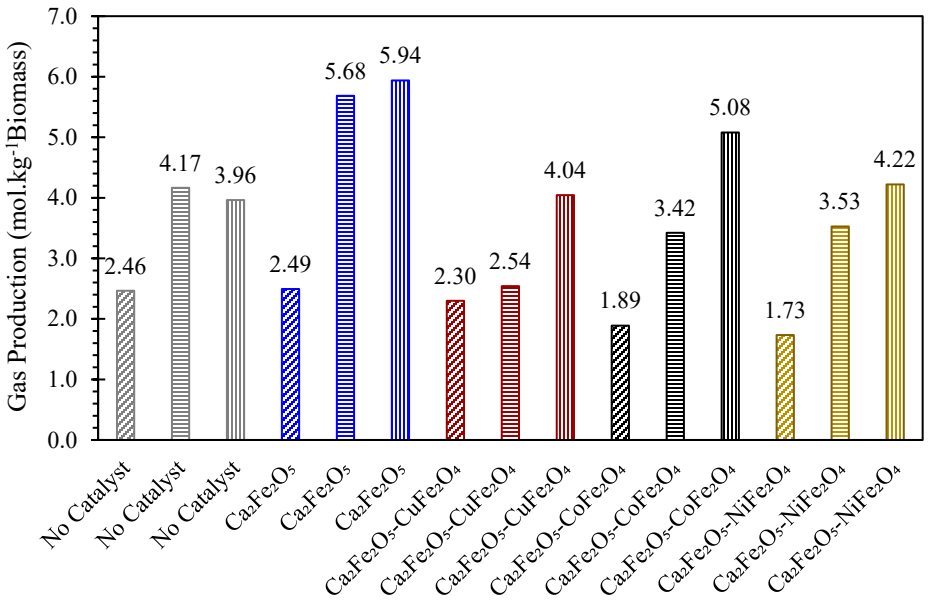

H_2

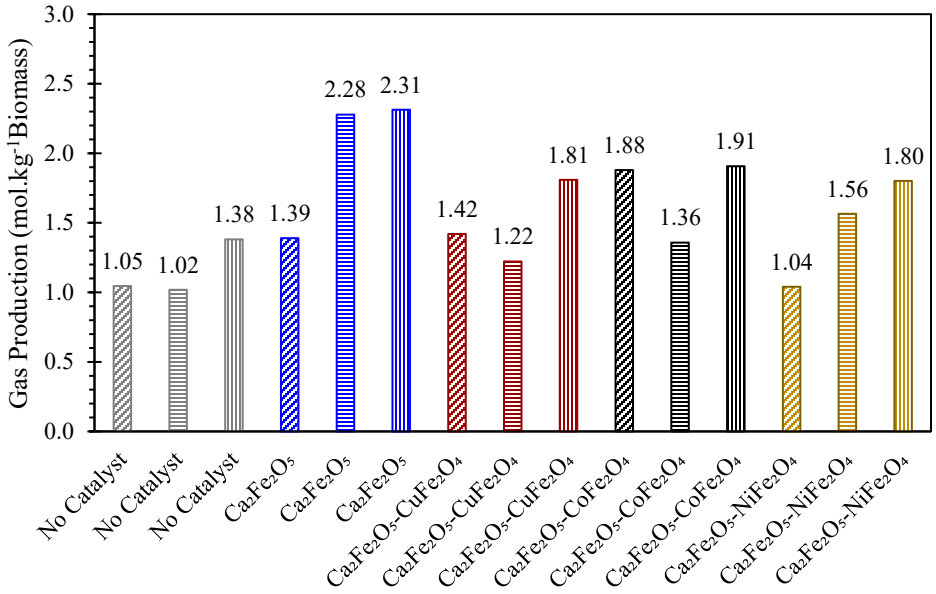
Gas Production (mol.kg-1Biomass)
3.0
2.5
2.0
1.5
1.0
0.5
0.0
1.05
1.02
1.38
1.39
2.28
2.31
1.42
1.22
1.81
1.88
1.36
1.91
1.04
1.56
1.80
No Catalyst
No Catalyst
No Catalyst
Ca2Fe2O5
Ca2Fe2O5
Ca2Fe2O5
Ca2Fe2O5-CuFe2O4
Ca2Fe2O5-CuFe2O4
Ca2Fe2O5-CuFe2O4
Ca2Fe2O5-CoFe2O4
Ca2Fe2O5-CoFe2O4
Ca2Fe2O5-CoFe2O4
Ca2Fe2O5-NiFe2O4
Ca2Fe2O5-NiFe2O4
Ca2Fe2O5-NiFe2O4

CO

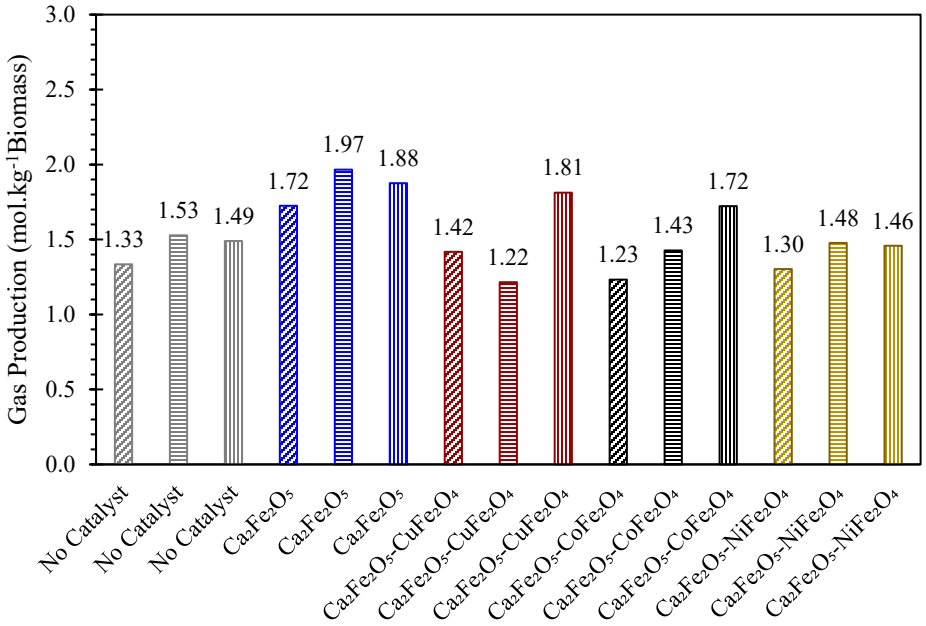
Gas Production (mol.kg-1Biomass)
3.0
2.5
2.0
1.5
1.0
0.5
0.0
1.33
1.53
1.49
1.72
1.97
1.88
1.42
1.22
1.81
1.23
1.43
1.72
1.30
1.48
1.46
No Catalyst
No Catalyst
No Catalyst
Ca2Fe2O5
Ca2Fe2O5
Ca2Fe2O5
Ca2Fe2O5-CuFe2O4
Ca2Fe2O5-CuFe2O4
Ca2Fe2O5-CuFe2O4
Ca2Fe2O5-CoFe2O4
Ca2Fe2O5-CoFe2O4
Ca2Fe2O5-CoFe2O4
Ca2Fe2O5-NiFe2O4
Ca2Fe2O5-NiFe2O4
Ca2Fe2O5-NiFe2O4

CH_4

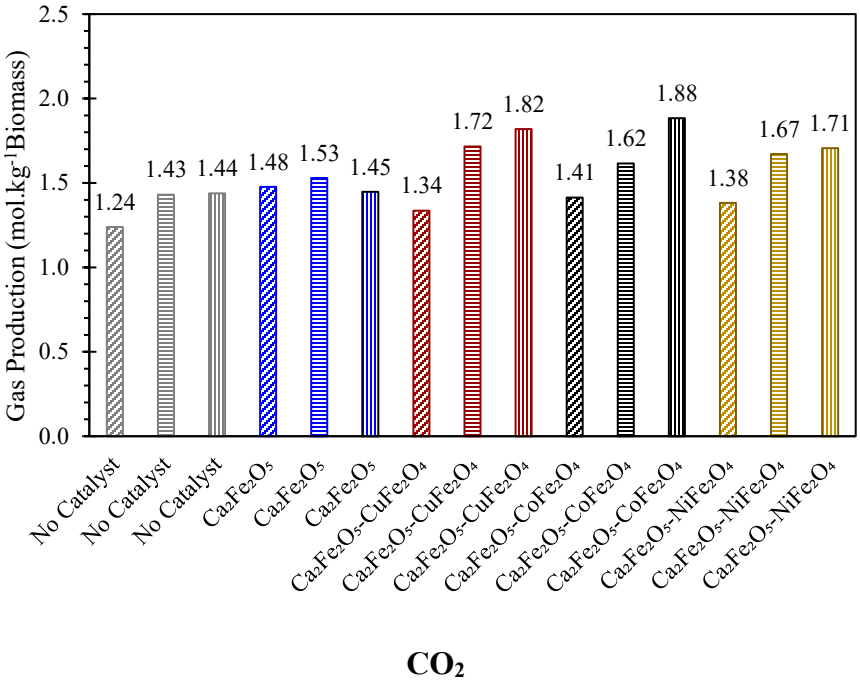

Figure 23. Effects of OCs on pyrolysis.

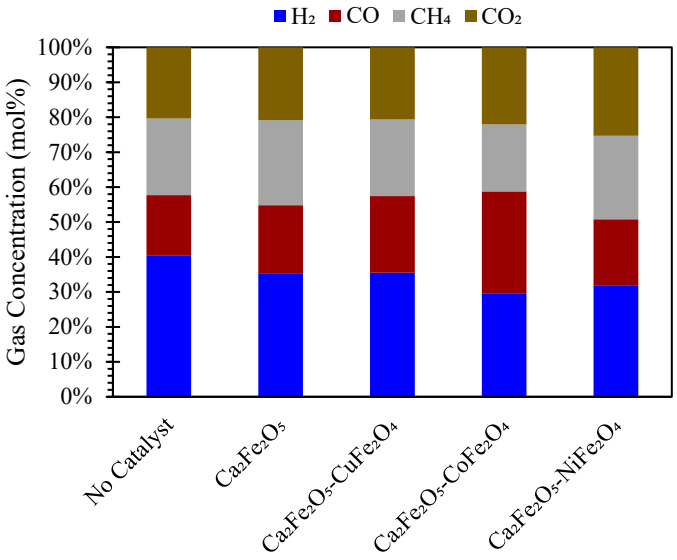
H₂ CO CH₄ CO₂
Gas Concentration (mol%)
100%
90%
80%
70%
60%
50%
40%
30%
20%
10%
0%
No Catalyst
Ca₂Fe₂O₅
Ca₂Fe₂O₅-CuFe₂O₄
Ca₂Fe₂O₅-CoFe₂O₄
Ca₂Fe₂O₅-NiFe₂O₄

a) 650℃

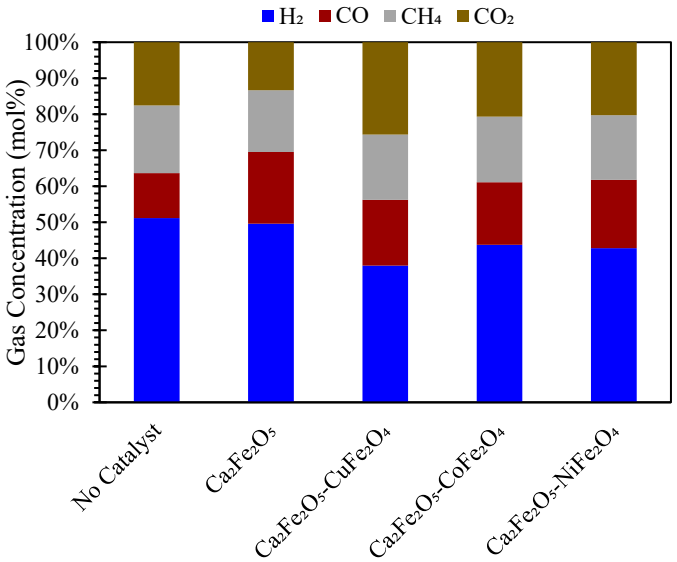
H₂ CO CH₄ CO₂
Gas Concentration (mol%)
100%
90%
80%
70%
60%
50%
40%
30%
20%
10%
0%
No Catalyst
Ca₂Fe₂O₅
Ca₂Fe₂O₅-CuFe₂O₄
Ca₂Fe₂O₅-CoFe₂O₄
Ca₂Fe₂O₅-NiFe₂O₄

b) 750℃

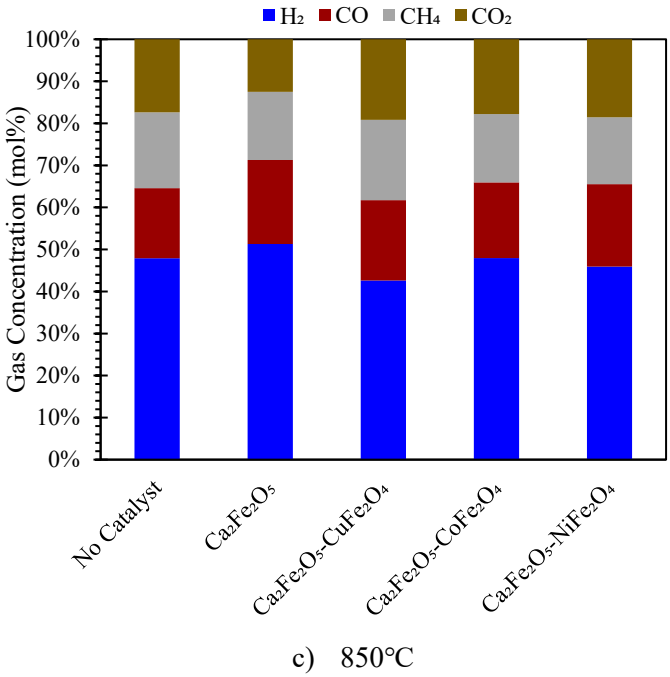

Figure 24. Temperature effect on pyrolysis.

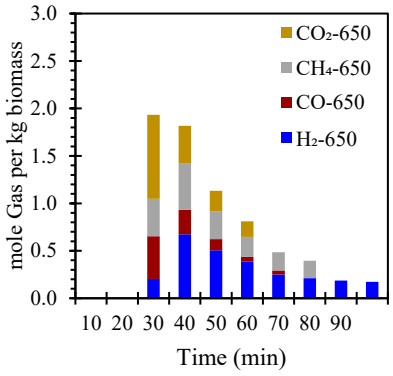

(a) No Catalyst, 650 °C

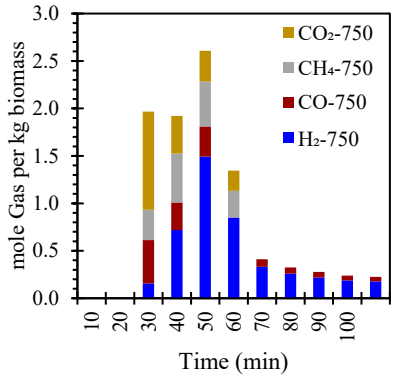

(a) No Catalyst, 750 °C

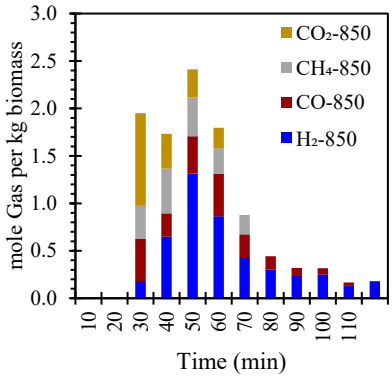

(a) No Catalyst, 850 °C

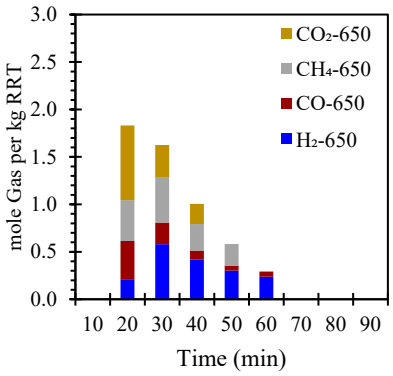

(b) $Ca_2Fe_2O_5$, 650 °C

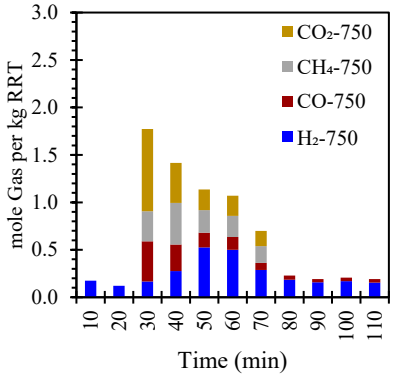

(b) $Ca_2Fe_2O_5$, 750 °C

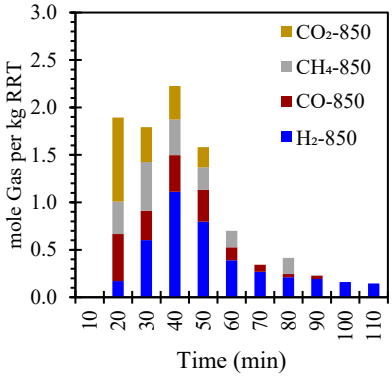

(b) $Ca_2Fe_2O_5$, 850 °C

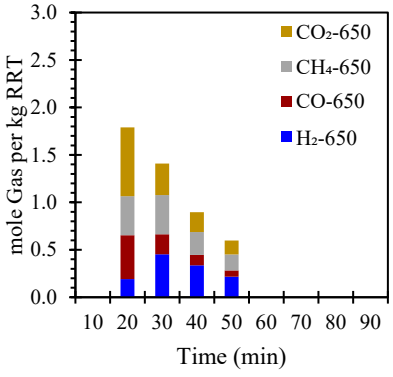

(c) $Ca_2Fe_2O_5$- $CuFe_2O_4$, 650 °C

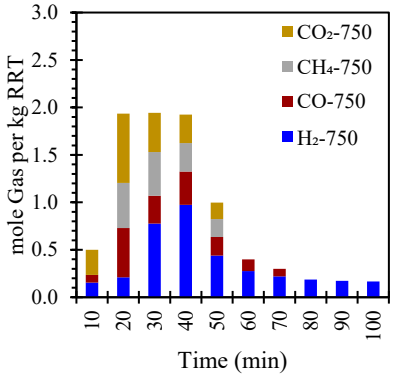

(c) $Ca_2Fe_2O_5$- $CuFe_2O_4$, 750 °C

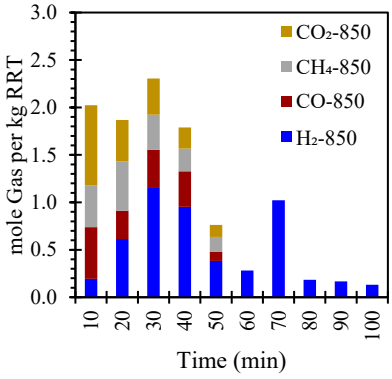

(c) $Ca_2Fe_2O_5$- $CuFe_2O_4$,850 °C

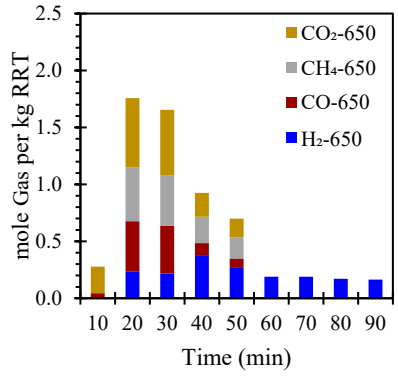

(d) $Ca_2Fe_2O_5$-$CoFe_2O_4$, 650 °C

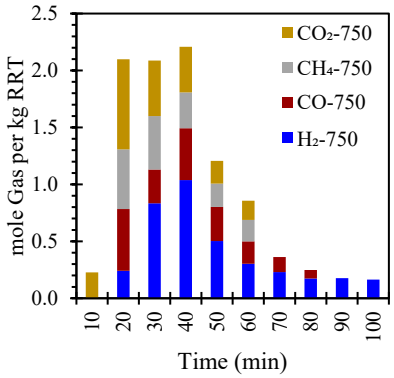

(d) $Ca_2Fe_2O_5$- $CoFe_2O_4$, 750 °C

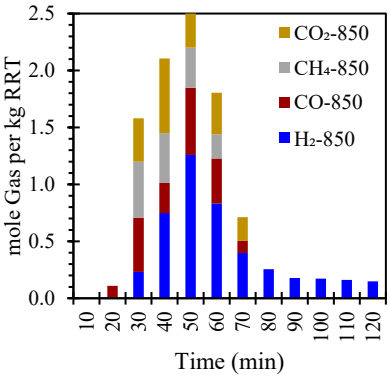

(d) $Ca_2Fe_2O_5$- $CoFe_2O_4$,850 °C

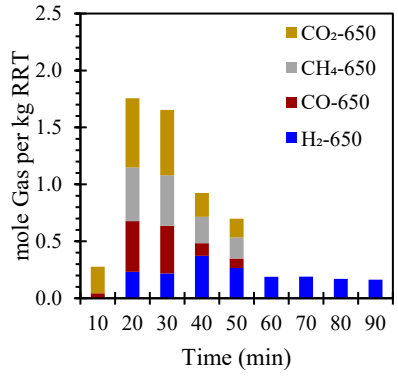

(e) $Ca_2Fe_2O_5$- $NiFe_2O_4$, 650 °C

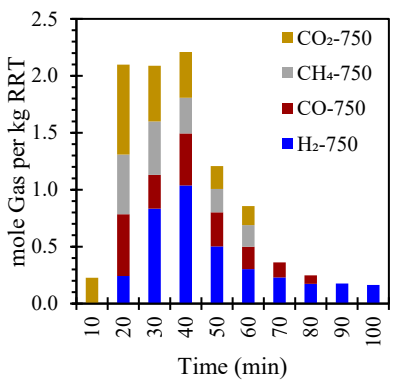

(e) $Ca_2Fe_2O_5$- $NiFe_2O_4$, 750 °C

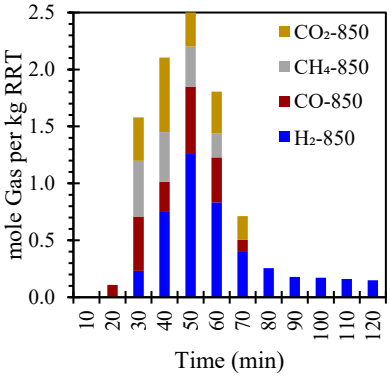

(e) $Ca_2Fe_2O_5$- $NiFe_2O_4$, 850 °C

Figure 25. Gas concentration over time.

4.5 CLG with gasifying agent

Gasification stands out as the most effective process to produce hydrogen from biomass. Syngas production and biomass gasification have roots dating back to before World War II [73]. In biomass gasification, carbon-rich materials are converted into a gaseous product called syngas, which is mostly composed of hydrogen (H_2) and carbon monoxide (CO), with smaller amounts of carbon dioxide (CO_2), and methane (CH_4). However, the syngas needs further separation to obtain pure hydrogen[74]. Thanks to its operation at high temperatures, gasification yields a greater amount of syngas compared to biochar and bio-oil. This versatile process enables the utilization of diverse carbon-based feedstocks (including natural gas, coal, petroleum, biomass, and industrial wastes). Different than pyrolysis the gasification process is further assisted by the gasifying agent steam with the corresponded flowrate of 0.1mL/min to increase the yield of syngas at different temperatures 650℃, 750℃, and 850℃.

While air might be the most readily available gasifying agent, steam (H_2O) offers distinct advantages in the biomass gasification process. By promoting hydrogen production, improving char utilization enhances efficiency and product quality. Furthermore, at lower temperatures of the process it enhances lower reaction temperatures because the steam participates in exothermic reactions (releases heat) that contribute to the overall process temperature. To access these advantages, it is necessary to consider the best injection rate for operating a steam-assisted gasification system. Figure 26 illustrates three distinct injection rates (0.05 mL/min, 0.1 mL/min, and 0.2 mL/min) for gasification. It is noted that with increasing temperature as well the injection rate, the concentration of H_2 rises from 20.01 to 28.34 mol.kg-1 kg at 850℃, indicating that the optimal steam injection rate is 0.2 mL/min. However, a notable portion of the injected

steam remained unreacted, which resulted in the dilution of bio-oil potential inefficiencies. Therefore, 0.1 mL/min was the chosen steam injection rate.

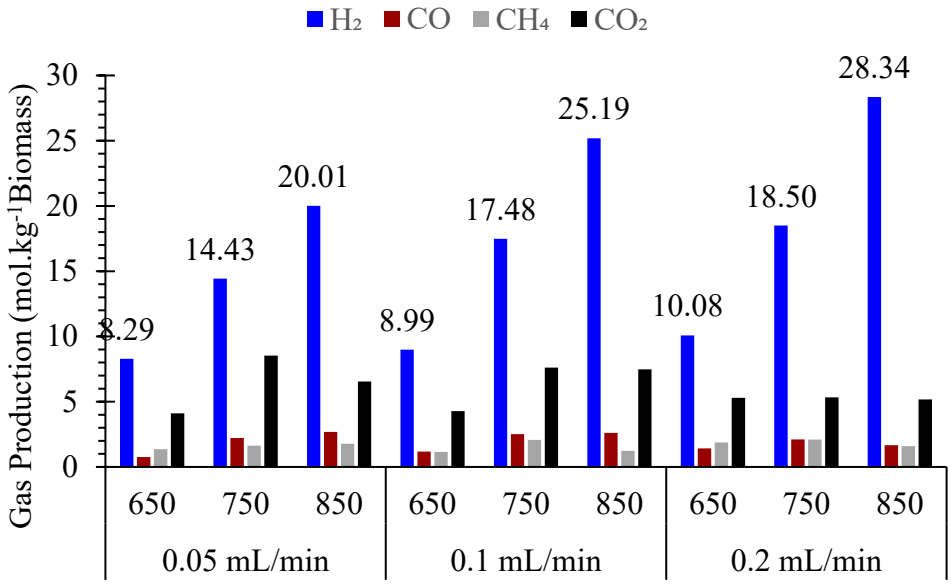

Figure 26. Best steam injection rate.

The first step on the gasification is the dehydration of biomass where moisture is evaporated even though prior gasification biomass undergoes in a pre-treatment process. Second it undergoes through a pyrolytic process where the volatile matter is first released resulting in vapors and char, followed by the cracking and reforming of the volatiles and the gasification of the char[73]. The introduction of steam and OC's effects can be seen in figure 26. Compared with pyrolysis the H_2 and CO_2 yield increased while CH_4 and CO decreased. This is due to series reactions, that includes water reacting with CO and C. It is notable the enhancement in H_2 in all variables compared to the pure RRT. Previously on the pyrolytic process $Ca_2Fe_2O_5$ demonstrated better performance with 5.94mol.kg^{-1} now with the addition of steam it is seen the rapid elevated H_2 production of 7.01mol.kg^{-1}. Furthermore, it is notorious that steam has made effect for the

subsequent gasification catalytic process due to the competing reactions. The reactions between volatiles and steam facilitated the production of gaseous products specially H_2 that includes char conversion, steam and dry reforming, catalyst regeneration, and water gas shift reactions that are shown below[27]:

***Steam oxidation of Fe^0*:** $2Fe + 2CaO + 3H_2O \rightarrow Ca_2Fe_2O_5 + 3H_2$ R34.

Steam tar reforming: $C_nH_m + 2nH_2O \rightarrow \left(n + \frac{m}{2}\right)H_2 + nCO_2$ R35.

Steam biochar reaction (primary): $C + H_2O \rightarrow CO + H_2$ R36.

Steam biochar reaction (secondary): $C + 2H_2O \rightarrow CO_2 + 2H_2$ R37.

Steam reforming: $CH_4 + H_2O \rightarrow CO + 3H_2$ **R38.**

Water gas shift: $CO + H_2O \rightarrow CO_2 + H_2$ **R39.**

Combustion reactions:

$CH_4 + 0.5O_2 \rightarrow CO + 2H_2$ **R40.**

$CH_4 + 2O_2 \rightarrow CO_2 + 2H_2O$ **R41.**

Tar reactions:

$tar + H_2O \rightarrow CO_2 + CO + H_2$ **R42.**

$tar + CO_2 \rightarrow CO + H_2O + H_2$ **R43.**

Methanation reactions:

$$C + 2H_2 \rightarrow CH_4 \quad \textbf{R44.}$$

$$2CO + 2H_2 \rightarrow CH_4 + CO_2 \quad \textbf{R45.}$$

From Fig. 27, it was observed that the temperature strongly affected the concentrations of the syngas components. Increase in temperature concentration of H_2, due to dominated endothermic reaction 36 and reaction 39 producing more H_2 and CO. The water gas shift and methanation reactions play crucial roles in facilitating CO_2 production, particularly the water gas shift, which promotes hydrogen peaks. At lower temperatures, where CO_2 concentrations are high due to these reactions, Figure 27a shows high CO_2 levels compared to those at 750 and 850°C. This disparity is attributed to the temperature favored competing Boudouard reaction (28), where CO_2 reacts with carbon to yield CO. The concentration of CO is influenced not only by the Boudouard reaction but also by the steam reaction with carbon (36) mostly. The rates of carbon oxidation reactions by steam and CO_2 are comparable, while the rate of the methanation reaction (reaction 45) is several orders of magnitude slower. Methane production predominantly occurs at lower temperatures, facilitated by the exothermic methanation reaction. However, as temperature increases, the rate of methanation reactions decreases, leading to a decline in CH_4 concentrations[75]. In catalytic pyrolysis, aside from syngas, bio-oil and biochar are generated and remain at the conclusion of the process. Conversely, gasification, due to its higher temperatures and the introduction of steam, promotes extensive reactions, leading to increased consumption of tar and char materials and resulting in elevated H_2 concentrations and overall syngas yield[73]. Hence, in the gasification process, higher temperatures, and steam introduction

prompt the release of more volatiles, facilitating reactions with char. The Steam oxidation of Fe^0 allows during this process to regenerate the catalyst that was previously reduced during the pyrolysis process producing more hydrogen as well.

In figure 29 it is possible to see how the steam has affected the concentration of gases. Compared to pyrolysis, it is in the initial moment that we start seeing peaks of H_2. It is notable how the gasifying steam accelerated the reactions rates and that even at the end is possible to pure hydrogen since that all the volatiles and char were previously consumed.

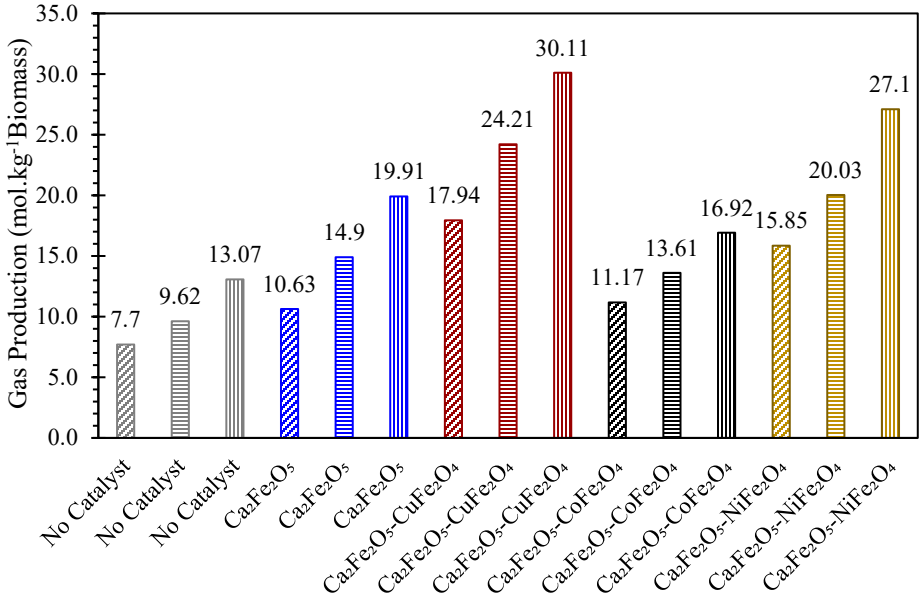

H_2

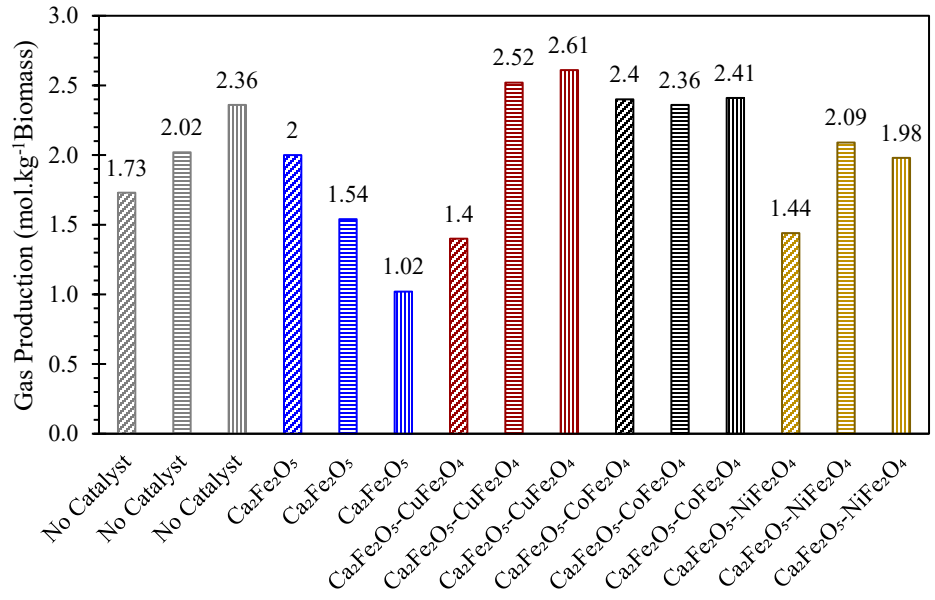
Gas Production (mol.kg-1Biomass)
3.0
2.5
2.0
1.5
1.0
0.5
0.0
1.73
2.02
2.36
2
1.54
1.02
1.4
2.52
2.61
2.4
2.36
2.41
1.44
2.09
1.98
No Catalyst
No Catalyst
No Catalyst
Ca2Fe2O5
Ca2Fe2O5
Ca2Fe2O5
Ca2Fe2O5-CuFe2O4
Ca2Fe2O5-CuFe2O4
Ca2Fe2O5-CuFe2O4
Ca2Fe2O5-CoFe2O4
Ca2Fe2O5-CoFe2O4
Ca2Fe2O5-CoFe2O4
Ca2Fe2O5-NiFe2O4
Ca2Fe2O5-NiFe2O4
Ca2Fe2O5-NiFe2O4

CO

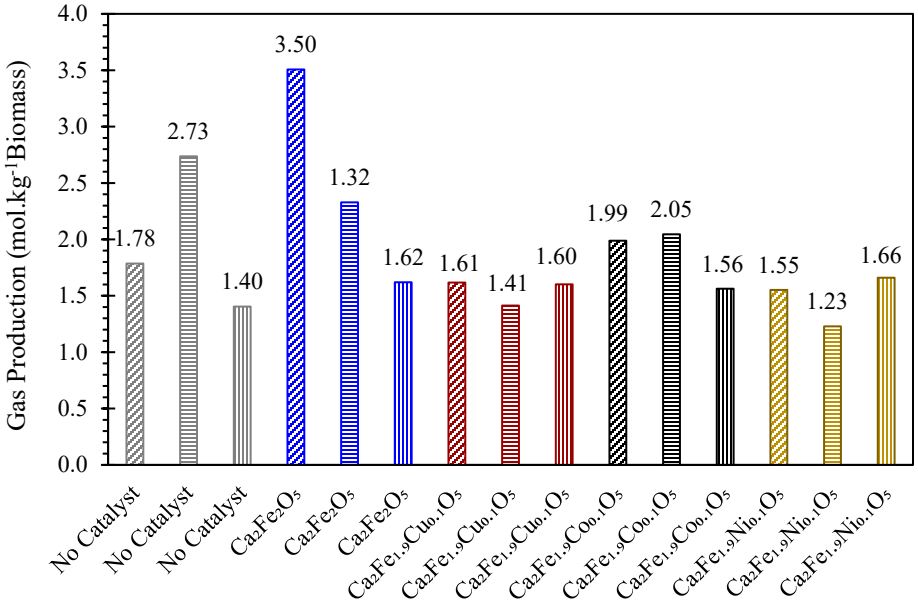
Gas Production (mol.kg-1Biomass)
4.0
3.5
3.0
2.5
2.0
1.5
1.0
0.5
0.0
1.78
2.73
1.40
3.50
1.32
1.62
1.61
1.41
1.60
1.99
2.05
1.56
1.55
1.23
1.66
No Catalyst
No Catalyst
No Catalyst
Ca2Fe2O5
Ca2Fe2O5
Ca2Fe2O5
Ca2Fe1.9Cu0.1O5
Ca2Fe1.9Cu0.1O5
Ca2Fe1.9Cu0.1O5
Ca2Fe1.9Co0.1O5
Ca2Fe1.9Co0.1O5
Ca2Fe1.9Co0.1O5
Ca2Fe1.9Ni0.1O5
Ca2Fe1.9Ni0.1O5
Ca2Fe1.9Ni0.1O5

CH_4

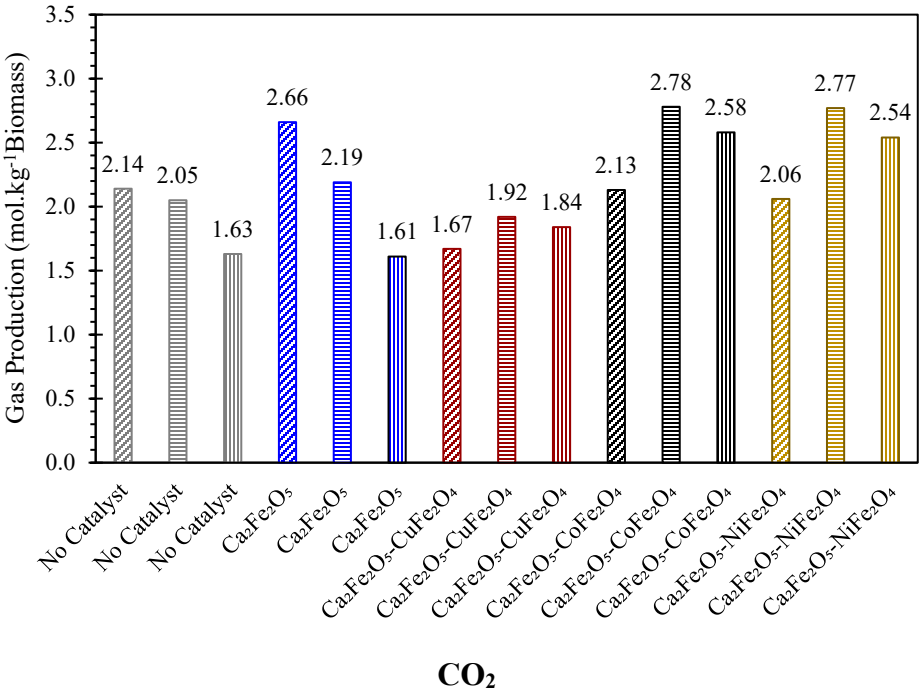

Figure 27. Effect of OCs in gasification.

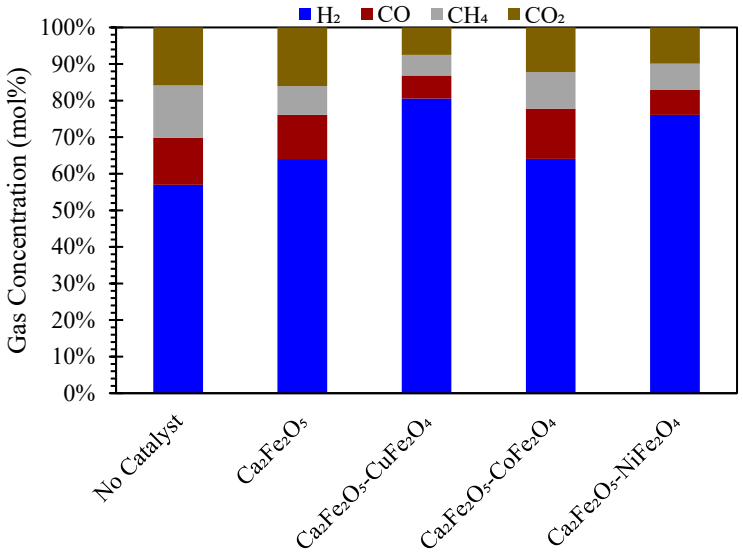

a) 650°C

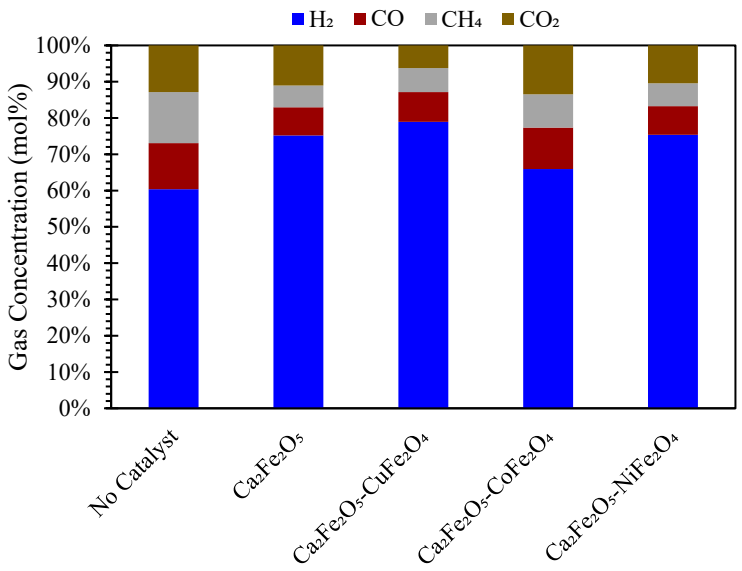

b) 750°C

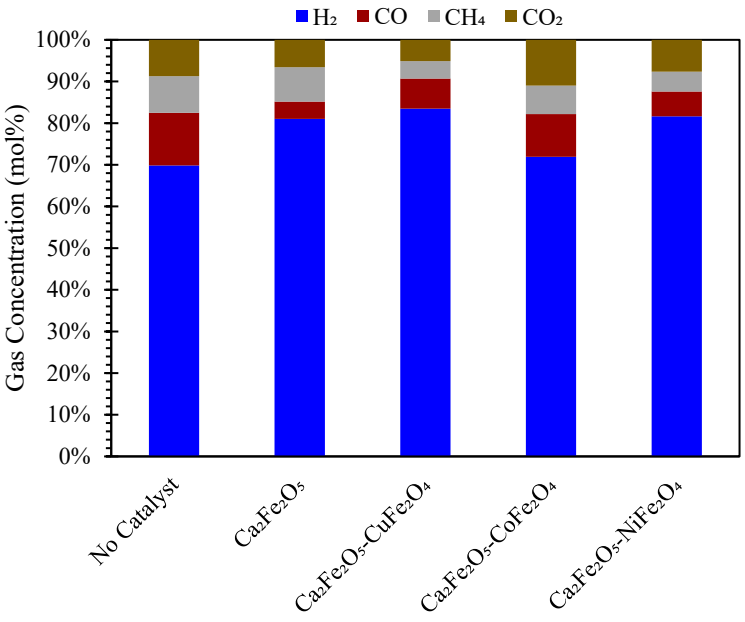

c) 850°C

Figure 28. Temperature effect in gasification.

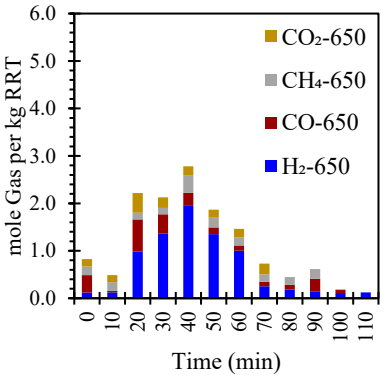

(a) No Catalyst, 650 °C

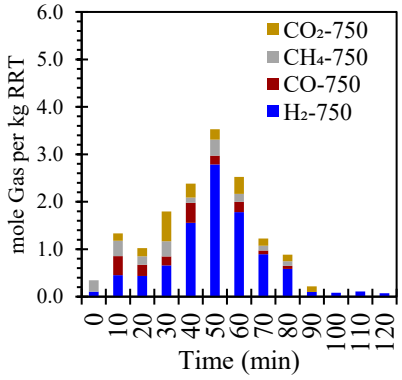

(a) No Catalyst, 750 °C

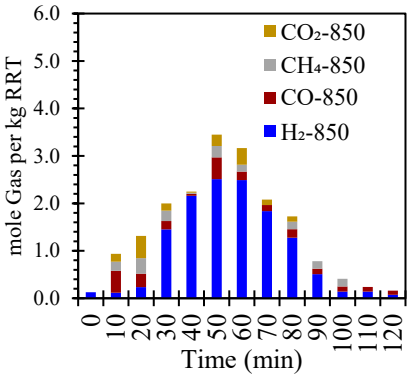

(a) No Catalyst, 850 °C

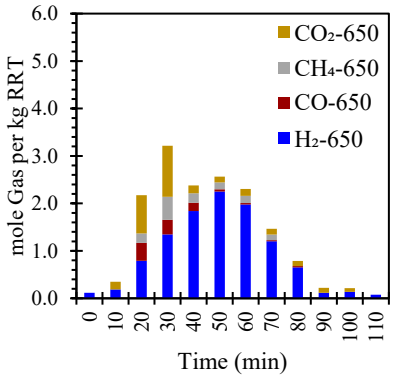

(b) $Ca_2Fe_2O_5$, 650 °C

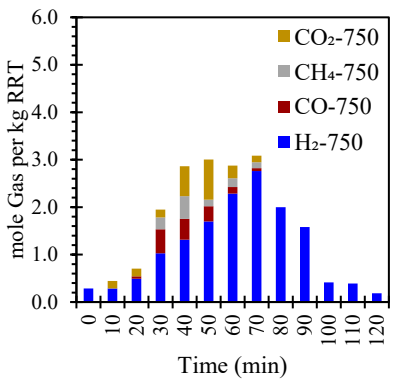

(b) $Ca_2Fe_2O_5$, 750 °C

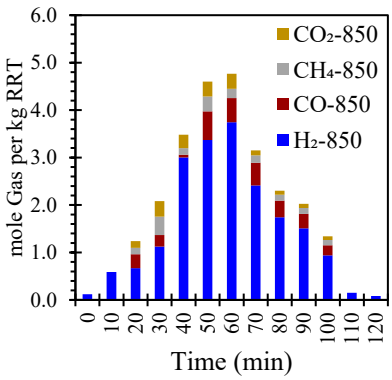

(b) $Ca_2Fe_2O_5$, 850 °C

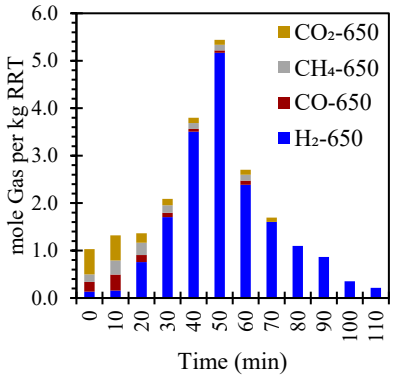

(c) $Ca_2Fe_2O_5$-$CuFe_2O_4$, 650 °C

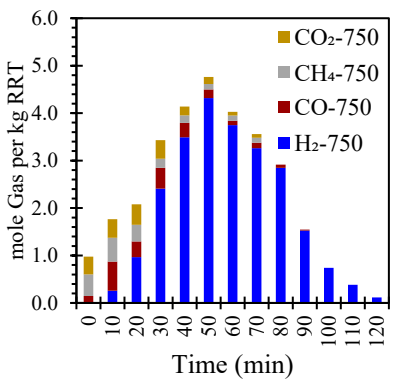

(c) $Ca_2Fe_2O_5$-$CuFe_2O_4$, 750 °C

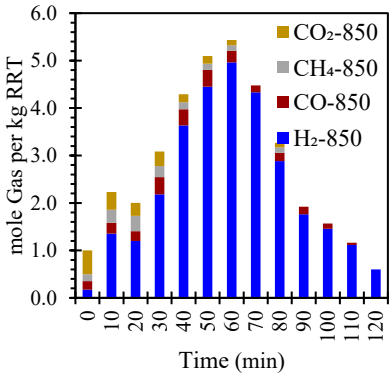

(c) $Ca_2Fe_2O_5$-$CuFe_2O_4$, 850°C

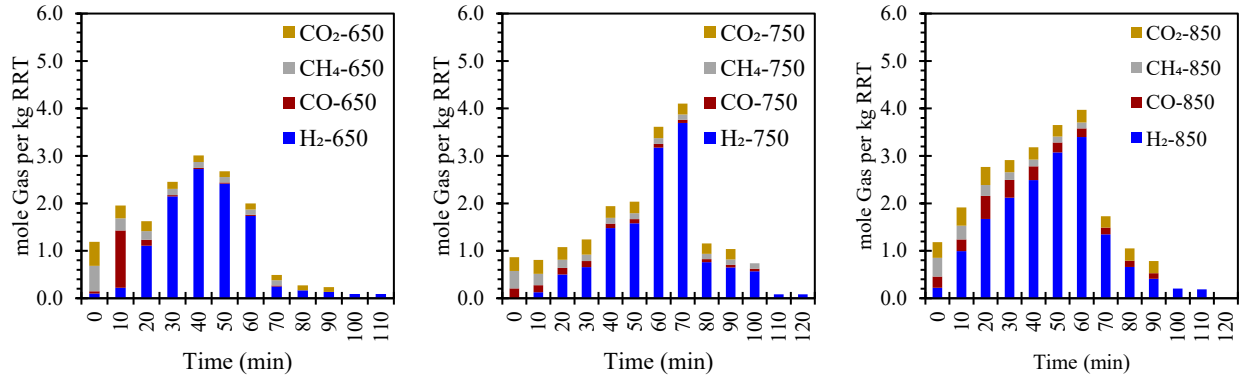

(d) $Ca_2Fe_2O_5$-$CoFe_2O_4$, 650 °C (d) $Ca_2Fe_2O_5$-$CoFe_2O_4$, 750 °C (d) $Ca_2Fe_2O_5$-$CoFe_2O_4$, 850 °C

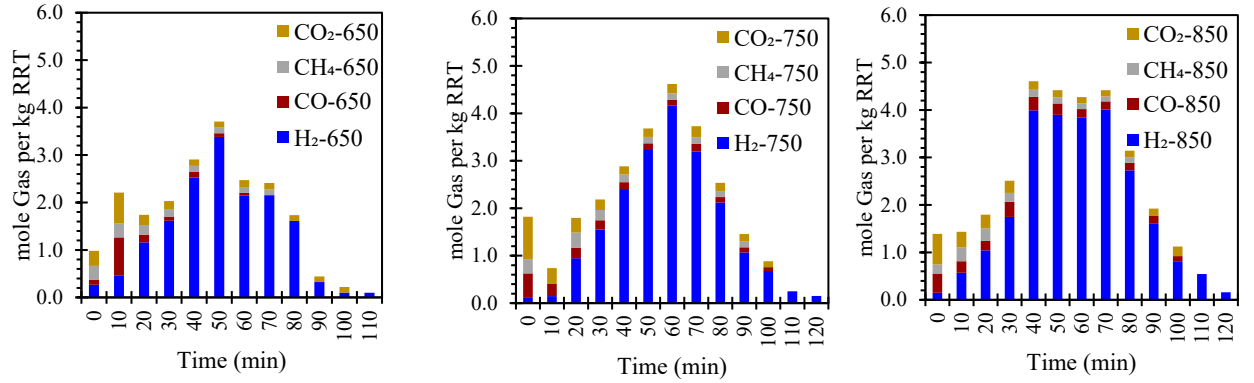

(e) $Ca_2Fe_2O_5$-$NiFe_2O_4$, 650 °C (e) $Ca_2Fe_2O_5$-$NiFe_2O_4$, 750 °C (e) $Ca_2Fe_2O_5$-$NiFe_2O_4$, 850 °C

Figure 29. Syngas gases concentration over time

4.6 Comparison between oxygen carriers

The synergy between steam and an oxygen carrier enhances hydrogen production by facilitating the steam-mediated re-oxidation of the reduced oxygen carrier. During pyrolysis, catalyst deactivation occurred due to reactions with gases inside the reactor. Among the catalysts tested, $Ca_2Fe_2O_5$ exhibited superior performance at this stage, yielding 4.71 mol/kg compared to pure RRT's 3.53 mol/kg. Other catalysts showed minimal impact. In gasification, oxygen carriers can be regenerated, leading to increased hydrogen production. In this process, $Ca_2Fe_2O_5$+$CuFe_2O_4$ demonstrated the highest hydrogen yield at 24.09 mol/kg, compared to pure RRT's 10.13 mol/kg. Following closely, $Ca_2Fe_2O_5$+$NiFe_2O_4$ yielded 20.99 mol/kg, while $Ca_2Fe_2O_5$ alone had negligible impact, and $Ca_2Fe_2O_5$-$CoFe_2O_4$ performed the poorest at 13.9 mol/kg. Additionally, biochar presence decreased gasification efficiency as it was consumed, promoting more hydrogen production. No biochar was detected at temperatures of 750 and 850 °C.

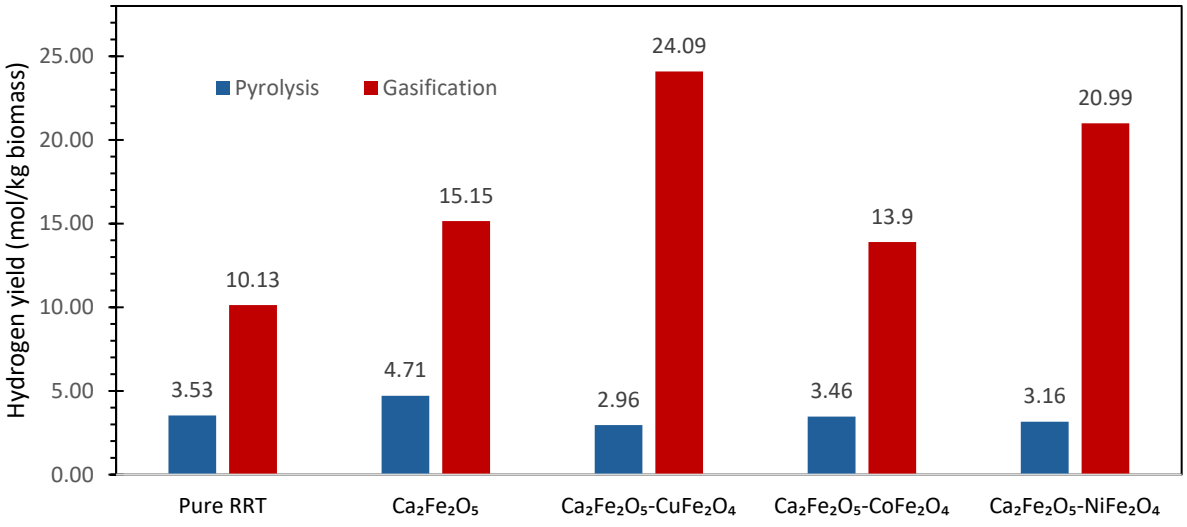

Figure 30. Catalyst performance during gasification and pyrolysis

5 Conclusion

On this study , chemical looping reforming was investigated on recycled Railroad ties biomass with $Ca_2Fe_2O_5$, $Ca_2Fe_2O_5$+$CuFe_2O_4$, $Ca_2Fe_2O_5$+$CoFe_2O_4$, and $Ca_2Fe_2O_5$+$NiFe_2O_4$ as the oxygen carriers to improve syngas production.

1. Different catalyst / OCs were synthesized by the Pechini method according to respective molar ratios. The SEM/EDS shows an even distribution of catalyst composition elements, explaining the impact of OCs on the chemical looping reforming. $Ca_2Fe_2O_5$+$CuFe_2O_4$ stands out for having the most uniform distribution of its constituent elements. TEM also shows the impact of good synthesis of the catalyst. All the components were present with their respective peaks. The characterization confirmed uniform elemental distribution, explaining the consistent influence of the oxygen carrier (OC) on gasification.
2. It was observed that a huge difference in pyrolysis and gasification results. In pyrolysis the cracking effect of the $Ca_2Fe_2O_5$ enhanced the production of syngas from 8.27 to 11.58mol.kg^{-1}. In the other hand, 0.1mL/min injection rate enhanced gasification reactions favoring the production of more H_2. A comparison between pyrolysis and gasification revealed that steam oxidation of the reduced OC significantly promoted H_2 production due to a synergistic reaction between steam and the OC. The application of a 0.1 mL/min steam injection rate significantly increased the H_2 yield by 87.7%.

3. The effect of temperature exhibited a consistent trend, with increasing temperature leading to a rise in H_2 yield for the gasification process. Mixing $Ca_2Fe_2O_5$ with $CuFe_2O_4$, and $NiFe_2O_4$ proved particularly effective, enhancing H_2 yield from 13.07 g/mol pure

RRT biomass to 30.11 g/mol biomass-$CuFe_2O_4$ and 27.1 g/mol biomass-$NiFe_2O_4$. Furthermore, $Ca_2Fe_2O_5$+$NiFe_2O_4$ also showed improvement in H_2 from 13.07mol.kg^{-1} to 27.1mol.kg^{-1} at 850℃ even though SEM shows that it didn't have a good distribution with is important for catalyst activation.

6 References

1. Johnston, B., M.C. Mayo, and A. Khare, *Hydrogen: the energy source for the 21st century.* Technovation, 2005. **25**(6): p. 569-585.
2. Rogelj, J. and R. Knutti, *Geosciences after Paris.* Nature Geoscience, 2016. **9**(3): p. 187-189.
3. Agency, I.E., *Net Zero by 2050. A roadmap for the Global Energy Sector*. 2021.
4. (IEA), I.E.A., *Global Hydrogen Review*. 2023.
5. (IEA), I.E.A., *The Future of Hydrogen. Seizing today's opportunities. .* June,2019.
6. Nikolaidis, P. and A. Poullikkas, *A comparative overview of hydrogen production processes.* Renewable and Sustainable Energy Reviews, 2017. **67**: p. 597-611.
7. Sehested, J., *Four challenges for nickel steam-reforming catalysts.* Catalysis Today, 2006. **111**(1): p. 103-110.
8. Sun, Z., et al., *Improvement of H2-rich gas production with tar abatement from pine wood conversion over bi-functional Ca2Fe2O5 catalyst: Investigation of inner-looping redox reaction and promoting mechanisms.* Applied Energy, 2018. **212**: p. 931-943.
9. Zhang, Y., et al., *A review of biomass pyrolysis gas: Forming mechanisms, influencing parameters, and product application upgrades.* Fuel, 2023. **347**: p. 128461.
10. Rafi, M., et al., *An overview of hydrogen generation by hydrolysis of Al and its alloys with the addition of carbon-based materials.* International Journal of Hydrogen Energy, 2023. **48**(56): p. 21345-21359.
11. Momirlan, M. and T.N. Veziroglu, *The properties of hydrogen as fuel tomorrow in sustainable energy system for a cleaner planet.* International Journal of Hydrogen Energy, 2005. **30**(7): p. 795-802.
12. Kothari, R., D. Buddhi, and R.L. Sawhney, *Comparison of environmental and economic aspects of various hydrogen production methods.* Renewable and Sustainable Energy Reviews, 2008. **12**(2): p. 553-563.
13. Ramachandran, R. and R.K. Menon, *An overview of industrial uses of hydrogen.* International Journal of Hydrogen Energy, 1998. **23**(7): p. 593-598.
14. Ajanovic, A., M. Sayer, and R. Haas, *The economics and the environmental benignity of different colors of hydrogen.* International Journal of Hydrogen Energy, 2022. **47**(57): p. 24136-24154.
15. Amin, M., et al., *Hydrogen production through renewable and non-renewable energy processes and their impact on climate change.* International Journal of Hydrogen Energy, 2022. **47**(77): p. 33112-33134.
16. Wang, G., et al., *A Review of Recent Advances in Biomass Pyrolysis.* Energy & Fuels, 2020. **34**(12): p. 15557-15578.
17. Vuppaladadiyam, A.K., et al., *Biomass pyrolysis: A review on recent advancements and green hydrogen production.* Bioresource Technology, 2022. **364**: p. 128087.
18. Muradov, N.Z., *Production of hydrogen from hydrocarbons*, in *Hydrogen Fuel*. 2008, CRC Press. p. 45-114.
19. Balthasar, W., *Hydrogen production and technology: today, tomorrow and beyond.* International Journal of Hydrogen Energy, 1984. **9**(8): p. 649-668.
20. Ahmad, M., et al., *Biochar as a sorbent for contaminant management in soil and water: A review.* Chemosphere, 2014. **99**: p. 19-33.

21. Chen, H.L., et al., *Review of plasma catalysis on hydrocarbon reforming for hydrogen production—Interaction, integration, and prospects.* Applied Catalysis B: Environmental, 2008. **85**(1): p. 1-9.
22. Navarro, R.M., M.A. Peña, and J.L.G. Fierro, *Hydrogen Production Reactions from Carbon Feedstocks: Fossil Fuels and Biomass.* Chemical Reviews, 2007. **107**(10): p. 3952-3991.
23. Holladay, J.D., et al., *An overview of hydrogen production technologies.* Catalysis Today, 2009. **139**(4): p. 244-260.
24. Ersöz, A., *Investigation of hydrocarbon reforming processes for micro-cogeneration systems.* International Journal of Hydrogen Energy, 2008. **33**(23): p. 7084-7094.
25. Neiva, L. and L. Gama, *A study on the characteristics of the reforming of methane: A review.* Brazilian Journal of Petroleum and Gas, 2010. **4**(3).
26. Ayabe, S., et al., *Catalytic autothermal reforming of methane and propane over supported metal catalysts.* Applied Catalysis A: General, 2003. **241**(1): p. 261-269.
27. Di Giuliano, A., et al., *Chemical Looping Combustion and Gasification: A Review and a Focus on European Research Projects.* Industrial & Engineering Chemistry Research, 2022. **61**(39): p. 14403-14432.
28. De Vos, Y., et al., *Sustainable iron-based oxygen carriers for Chemical Looping for Hydrogen Generation.* International Journal of Hydrogen Energy, 2019. **44**(3): p. 1374-1391.
29. Spallina, V., et al., *Integration of Coal Gasification and Packed Bed CLC process for High Efficiency and Near-zero Emission Power Generation.* Energy Procedia, 2013. **37**: p. 662-670.
30. Erlach, B., M. Schmidt, and G. Tsatsaronis, *Comparison of carbon capture IGCC with pre-combustion decarbonisation and with chemical-looping combustion.* Energy, 2011. **36**(6): p. 3804-3815.
31. Khan, M.N. and T. Shamim, *Investigation of hydrogen generation in a three reactor chemical looping reforming process.* Applied Energy, 2016. **162**: p. 1186-1194.
32. Ishida, M., D. Zheng, and T. Akehata, *Evaluation of a chemical-looping-combustion power-generation system by graphic exergy analysis.* Energy, 1987. **12**: p. 147-154.
33. Zhu, X., et al., *Chemical looping beyond combustion – a perspective.* Energy & Environmental Science, 2020. **13**(3): p. 772-804.
34. Yao, P., et al., *Application of machine learning in carbon capture and storage: An in-depth insight from the perspective of geoscience.* Fuel, 2023. **333**: p. 126296.
35. Chopra, S., *A Mechanistic Analysis of Particle Flow in a Multiphase Chemical Looping Reactor with Theories of Contact Mechanics.* 2023.
36. Li, D., et al., *Chemical Looping Conversion of Gaseous and Liquid Fuels for Chemical Production: A Review.* Energy & Fuels, 2020. **34**(5): p. 5381-5413.
37. Dawa, T. and B. Sajjadi, *Exploring the potential of perovskite structures for chemical looping technology: A state-of-the-art review.* Fuel Processing Technology, 2024. **253**: p. 108022.
38. Adánez, J. and A. Abad, *Chemical-looping combustion: Status and research needs.* Proceedings of the Combustion Institute, 2019. **37**(4): p. 4303-4317.
39. Czakiert, T., et al., *Chemical looping combustion: a brief overview.* Energies, 2022. **15**(4): p. 1563.

40. Adanez, J., et al., *Progress in chemical-looping combustion and reforming technologies.* Progress in energy and combustion science, 2012. **38**(2): p. 215-282.
41. Aouad, S., et al., *A review on the dry reforming processes for hydrogen production: catalytic materials and technologies.* Catal. Mater. Hydrog. Prod. Electro Oxid. React. Front. Ceram. Sci, 2018. **2**: p. 60-128.
42. Rydén, M., A. Lyngfelt, and T. Mattisson, *Chemical-Looping Combustion and Chemical-Looping Reforming in a Circulating Fluidized-Bed Reactor Using Ni-Based Oxygen Carriers.* Energy & Fuels, 2008. **22**(4): p. 2585-2597.
43. Roshan Kumar, T., et al., *Process Analysis of Chemical Looping Gasification of Biomass for Fischer–Tropsch Crude Production with Net-Negative CO2 Emissions: Part 1.* Energy & Fuels, 2022. **36**(17): p. 9687-9705.
44. Mattisson, T., et al., *Chemical-looping technologies using circulating fluidized bed systems: Status of development.* Fuel Processing Technology, 2018. **172**: p. 1-12.
45. Cao, Y., et al., *On the kinetics of Mn2O3/ZrO2 oxygen carrier for chemical looping air separation.* Chemical Engineering and Processing - Process Intensification, 2019. **136**: p. 82-91.
46. Hallberg, P., et al., *Chemical Looping Combustion and Chemical Looping with Oxygen Uncoupling Experiments in a Batch Reactor Using Spray-Dried CaMn1–xMxO3−δ (M = Ti, Fe, Mg) Particles as Oxygen Carriers.* Energy & Fuels, 2013. **27**(3): p. 1473-1481.
47. Mattisson, T., *Materials for Chemical-Looping with Oxygen Uncoupling.* ISRN Chemical Engineering, 2013. **2013**: p. 526375.
48. Huang, Z., et al., *Evaluation of multi-cycle performance of chemical looping dry reforming using CO2 as an oxidant with Fe–Ni bimetallic oxides.* Journal of Energy Chemistry, 2016. **25**(1): p. 62-70.
49. Huang, Z., et al., *Investigation on reactivity of iron nickel oxides in chemical looping dry reforming.* Energy, 2016. **116**: p. 53-63.
50. Cheng, Z. and J. Lin, *Layered organic–inorganic hybrid perovskites: structure, optical properties, film preparation, patterning and templating engineering.* CrystEngComm, 2010. **12**(10): p. 2646-2662.
51. Giovanni, D., *Optical-spin dynamics in organic-inorganic lead halide perovskites*. 2017.
52. Ono, L.K., E.J. Juarez-Perez, and Y. Qi, *Progress on Perovskite Materials and Solar Cells with Mixed Cations and Halide Anions.* ACS Applied Materials & Interfaces, 2017. **9**(36): p. 30197-30246.
53. Green, M.A., A. Ho-Baillie, and H.J. Snaith, *The emergence of perovskite solar cells.* Nature Photonics, 2014. **8**(7): p. 506-514.
54. Lozano, G., *The Role of Metal Halide Perovskites in Next-Generation Lighting Devices.* The Journal of Physical Chemistry Letters, 2018. **9**(14): p. 3987-3997.
55. Xu, J., et al., *Three-dimensionally ordered macroporous LaCoxFe1−xO3 perovskite-type complex oxide catalysts for diesel soot combustion.* Catalysis Today, 2010. **153**(3): p. 136-142.
56. He, F., et al., *The use of La1−xSrxFeO3 perovskite-type oxides as oxygen carriers in chemical-looping reforming of methane.* Fuel, 2013. **108**: p. 465-473.
57. Jiang, Y., et al., *Oxygen Storage Characteristics and Redox Behaviors of Lanthanum Perovskite Oxides with Transition Metals in the B-Sites.* Energy & Fuels, 2023. **37**(13): p. 9419-9433.

58. Jha, S., et al., *A Review of Biomass Resources and Thermochemical Conversion Technologies.* Chemical Engineering & Technology, 2022. **45**(5): p. 791-799.
59. Chen, F., et al., *Characteristics and catalytic properties of Ni/CaAlOx catalyst for hydrogen-enriched syngas production from pyrolysis-steam reforming of biomass sawdust.* Applied Catalysis B: Environmental, 2016. **183**: p. 168-175.
60. Duman, G., M.A. Uddin, and J. Yanik, *Hydrogen production from algal biomass via steam gasification.* Bioresource Technology, 2014. **166**: p. 24-30.
61. Richardson, Y., et al., *In situ generation of Ni metal nanoparticles as catalyst for H2-rich syngas production from biomass gasification.* Applied Catalysis A: General, 2010. **382**(2): p. 220-230.
62. Díaz-Rey, M.R., et al., *Hydrogen-rich gas production from algae-biomass by low temperature catalytic gasification.* Catalysis Today, 2015. **257**: p. 177-184.
63. Bergmann, F., *Process for the production of calcium carbide in blast furnaces.* German patent, 1897. **29**: p. 384.
64. Sun, Z., et al., *Ca2Fe2O5: A promising oxygen carrier for CO/CH4 conversion and almost-pure H2 production with inherent CO2 capture over a two-step chemical looping hydrogen generation process.* Applied Energy, 2018. **211**: p. 431-442.
65. Chen, L., et al., *Performance of Ce-modified V-W-Ti type catalyst on simultaneous control of NO and typical VOCS.* Fuel Processing Technology, 2020. **207**: p. 106483.
66. Shafizadeh, F., *Introduction to pyrolysis of biomass.* Journal of Analytical and Applied Pyrolysis, 1982. **3**(4): p. 283-305.
67. Garcia-Perez, M., et al., *Fast Pyrolysis of Oil Mallee Woody Biomass: Effect of Temperature on the Yield and Quality of Pyrolysis Products.* Industrial & Engineering Chemistry Research, 2008. **47**(6): p. 1846-1854.
68. Xie, Q., et al., *Syngas production by two-stage method of biomass catalytic pyrolysis and gasification.* Bioresource Technology, 2012. **110**: p. 603-609.
69. Parthasarathy, P., et al., *Influence of process conditions on product yield of waste tyre pyrolysis-A review.* Korean Journal of Chemical Engineering, 2016. **33**: p. 2268-2286.
70. Chen, J., et al., *Reaction schemes of barium ferrite in biomass chemical looping gasification for hydrogen-enriched syngas generation via an outer-inner looping redox reaction mechanism.* Energy Conversion and Management, 2019. **189**: p. 81-90.
71. Guo, F., et al., *Catalytic cracking of biomass pyrolysis tar over char-supported catalysts.* Energy Conversion and Management, 2018. **167**: p. 81-90.
72. Chen, J., et al., *Identifying the roles of MFe2O4 (M=Cu, Ba, Ni, and Co) in the chemical looping reforming of char, pyrolysis gas and tar resulting from biomass pyrolysis.* International Journal of Hydrogen Energy, 2019. **44**(10): p. 4674-4687.
73. Ahmad, A.A., et al., *Assessing the gasification performance of biomass: A review on biomass gasification process conditions, optimization and economic evaluation.* Renewable and Sustainable Energy Reviews, 2016. **53**: p. 1333-1347.
74. Lider, A., et al., *Materials and techniques for hydrogen separation from methane-containing gas mixtures.* International Journal of Hydrogen Energy, 2023. **48**(73): p. 28390-28411.
75. Tilay, A., et al., *Gasification of canola meal and factors affecting gasification. Process Bioenerg Res 7: 1131–1143*. 2014.